ARDB Technical Note

Switched Matrix Accelerator

D. H. Whittum

In this technical note we describe the concept of a structure that provides acceleration for multiple bunches, and a short exposure time for any single copper surface. Scalings are set down, results of circuit simulations are noted.

Introduction

Conventional accelerating structures are *passive* devices, achieving large fields by means of resonant excitation, over a long time scale, of order the natural decrement time for fields due to wall losses. Such structures are ultimately limited in achievable field due to the phenomenon of wall heating in a single pulse ("pulsed heating"), that results in a wall temperature rise varying in proportion to incident power density and the square root of the exposure time. Reduction of exposure time at fixed power density can only be accomplished at the expense of a reduction in the field. Moreover, for collider applications, a large number of particle bunches is required, and this in itself would appear to require long exposure times for copper.

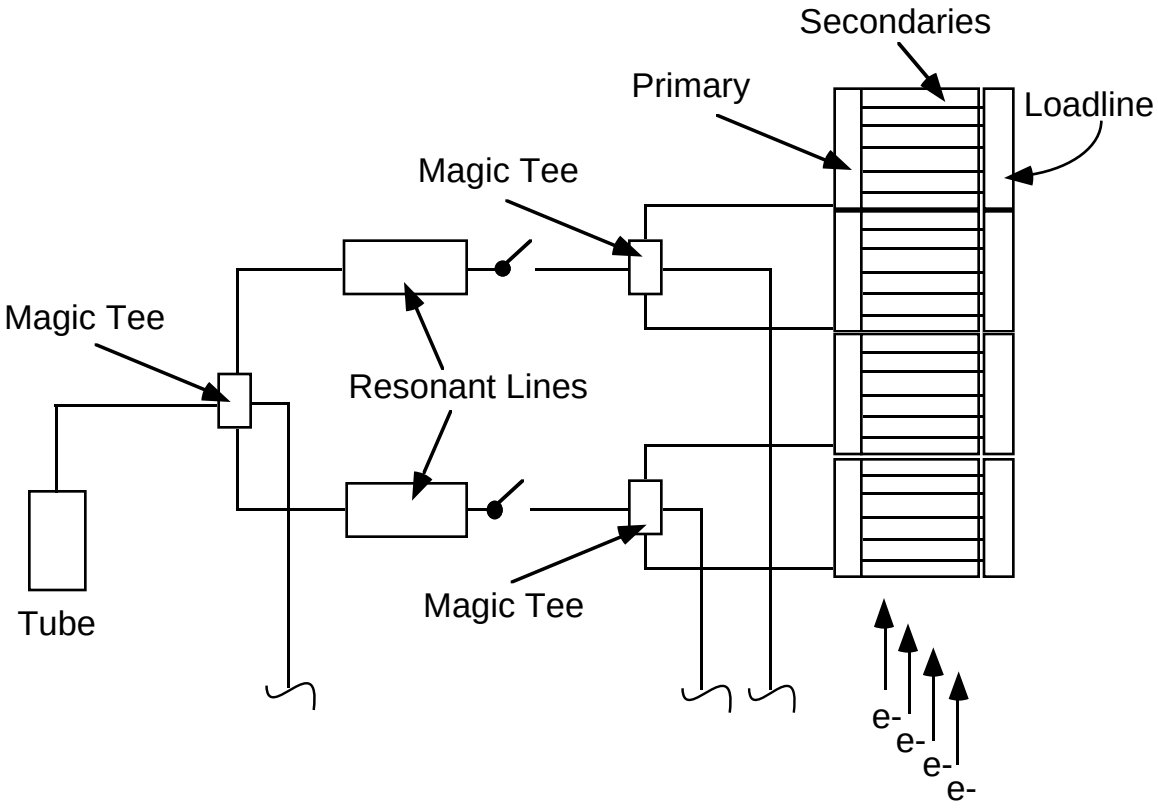

Fig. 1. Scheme for one tube-station of a high-gradient W-Band linac. Active high-power microwave switches will be essential components.

In this note we describe an accelerator concept that achieves resonant energy storage, short exposure time in the accelerating structure itself, and multi-bunch acceleration. The concept is premised on a high-power rf switch, and a matrix of acceleration cavities, rather than a linear array as in conventional travelling wave structures.

Here we set down the basic design considerations for an active matrix accelerator at W-Band (91.39GHz or "32 x SLAC"). In Sec.1 we outline the concept and the basic macroscopic circuit parameters characterizing its performance. In Sec. 2 we analyze in detail the transient features of the device that are fundamental to its operation. In Sec. 3 we offer conclusions as to additional problems of interest. An important subject not addressed in this note is the detailed design of copper and switch dimensions; we leave this to a later note.

1. Scaling Laws for a Matrix Accelerator

For the sake of definiteness we depict one tube-station in Fig.1, consisting of a power amplifier, a microwave network, incorporating an active pulse compression system, and accelerating structures. Figure 1 shows one tube with feed split by a hybrid-tee, each arm charging a resonant delay line. These lines are *Q*-switched by an active high-power microwave switch, and the output of each is split by a magic-tee to feed a total of four accelerating structures. The subject of this note is the structure. A detail of the schematic for one such structure is depicted in Fig. 2.

In Fig. 2 we see a "primary" transmission line being filled with power from the output of the *Q*-switched resonant line. Following the charging of the primary line, each primary cell is discharged down the corresponding secondary line, as indicated in Fig. 3. This primary line serves the purpose of power distribution, and additional pulse compression, taking a 200MW, 10ns pulse from the network, and breaking it into many sub-ns pulses for distribution down the 50 or so secondary transmission lines.

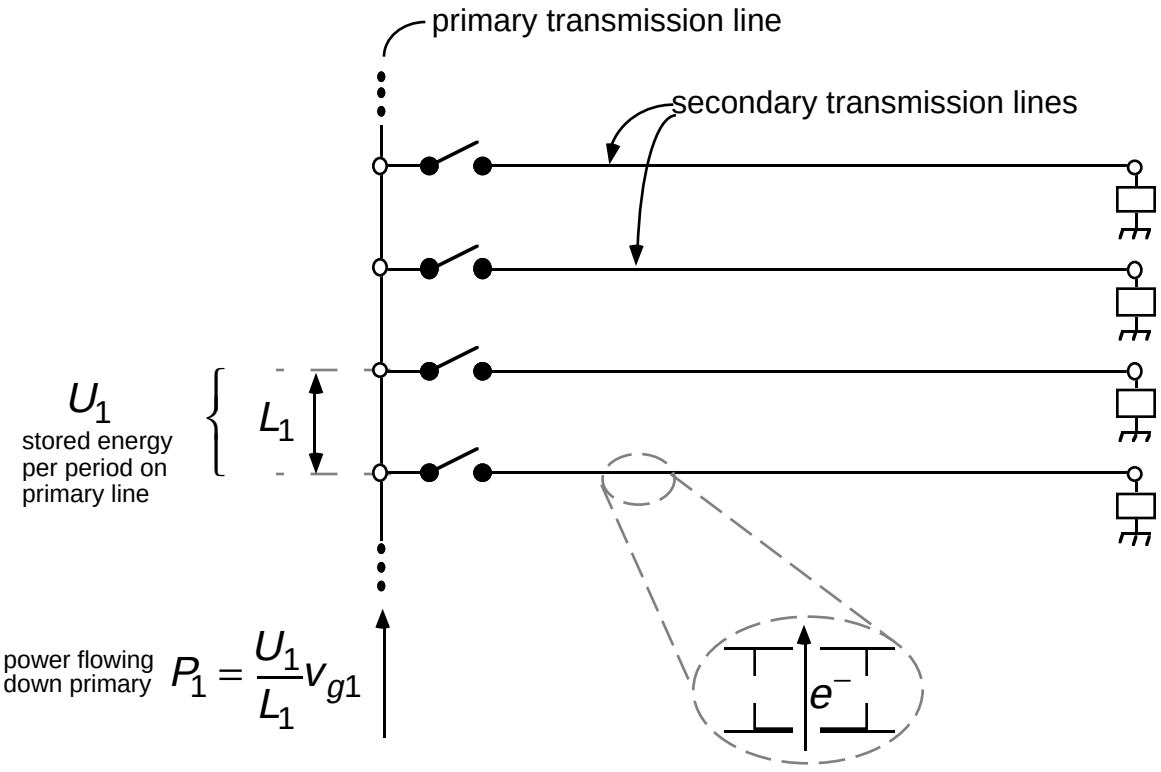

Fig. 2 Active matrix accelerator during charge-up.

1.1 Primary Transmission Line

The primary line is filled with input power P_1, corresponding to stored energy U_1 per period, determined by the group velocity V_{g1}, and the period length L_1. As seen in Fig. 3, after charge-up of the primary, a switch is closed discharging each period of the primary into a secondary transmission line. The secondary consists of a quasi-periodic array of accelerating cavities and the voltage in each cell is determined by the stored energy in a cell, U_2. This energy is in turn determined by the period length L_2, the group velocity on the secondary line V_{g2}, and the incident power.

For the present discussion, the primary transmission line will be taken to be an iris loaded rectangular waveguide terminated in a matched load, as indicated in Fig. 4. (The subject of a standing-wave primary, and use of other geometries and modes is being studied.) From the point of view of circuit analysis, the rectangular geometry has the virtue of coupling in a transparent manner, after switch closure, where each cell has the appearance of TE_{10} waveguide, iris coupled into a periodically-loaded TE_{10} waveguide. The length (w_1 in Fig. 4) of a primary cell will be 10-20 half-wavelengths.

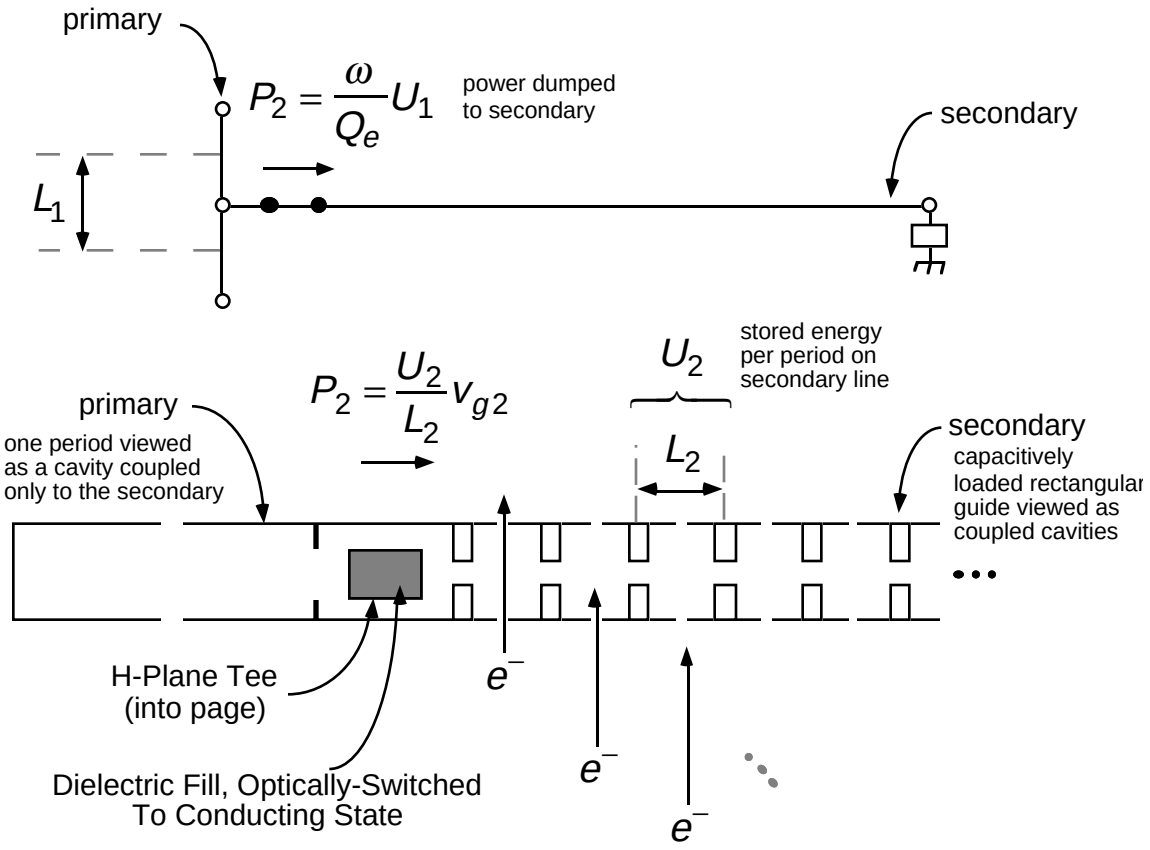

Fig. 3 Active matrix during discharge and acceleration.

We will take the cell-length L_1 in the primary to be constant. This is for simplicity. In general, this cell-length is not a completely free parameter insofar as synchronism between the rf and the beam imposes a requirement on phase-advance per cell θ_1 in the primary,

$$\frac{\omega L_1}{c} = \theta_1.$$

Thus constant cell-length and constant phase-advance per cell are equivalent assumptions. In principle one could flout this at the expense of some additional variety in the interconnect between primary and secondary, but for simplicity we fix this condition for the present work. In addition, we ask that the stored energy per unit length be constant throughout the primary. This implies that the primary scalings are those typically applied to a constant gradient accelerating structure, and may be summarized as follows. Let there be N_1 cells in the primary, and denote the initial group velocity $V_{g1}(0)$, then

$$V_{g1}(0) = \frac{\omega N_1 L_1}{Q_{w1}}\left(1 - e^{-2\tau_1}\right)^{-1},$$

with Q_{w1} the wall Q of one primary cell, and t_1 the attenuation parameter for the primary line. The power flowing through the primary at location y , and the group velocity at this location are then given by

$$\frac{V_{g1}(y)}{V_{g1}(0)} = \frac{P_1(y)}{P_1(0)} = 1 - \frac{y}{N_1 L_1}\left(1 - e^{-2\tau_1}\right).$$

The stored energy per cell may be determined from the input power $P_1(0)$, according to

$$U_1 = \frac{P_1(0) L_1}{V_{g1}(0)}.$$

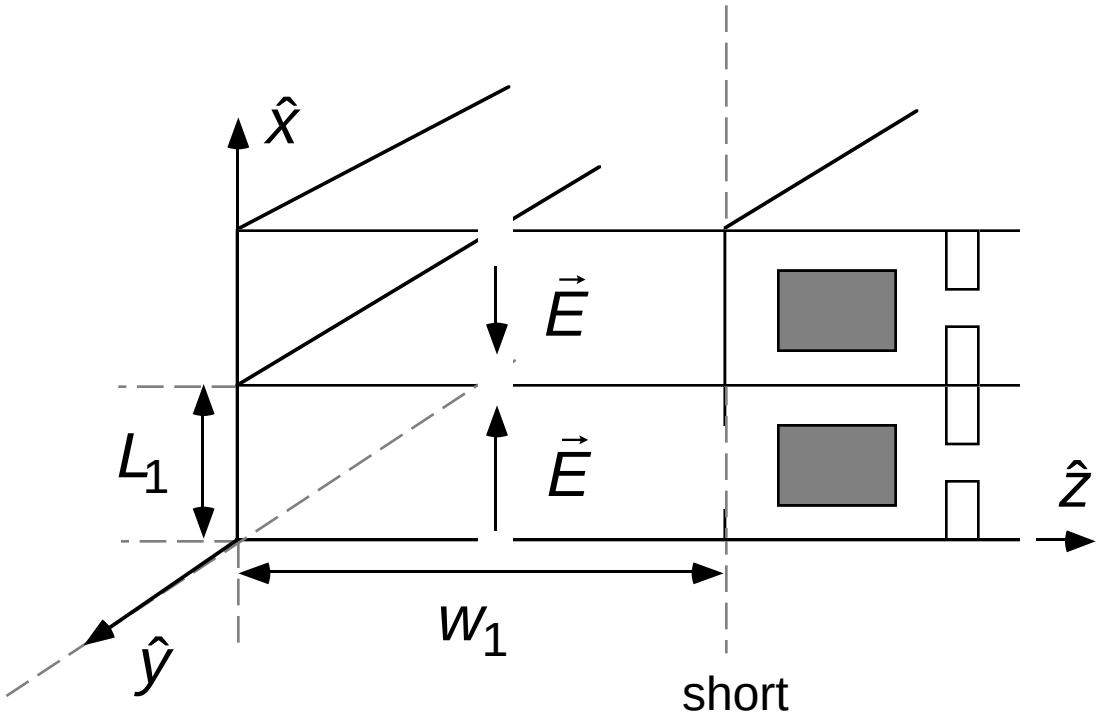

Fig. 4 Loaded-rectangular geometry for the primary transmission line. The plane marked "short" is a virtual short, presented by the tuned *H*-plane tee. This tee extends into the page, with footprint marked by the cross-hatced area. The photo-conducting fill in the *H*-plane tee, when switched modifies the impedance looking into the secondary, providing a match, and discharge of the primary cell. On this discharge time-scale, primary cells are viewed as being uncoupled.

1.2 Calculations for a Rectangular Pillbox

Important inputs to both the primary and secondary scalings are the basic scalings for a rectangular pillbox resonator. The picture is that of Fig. 5.

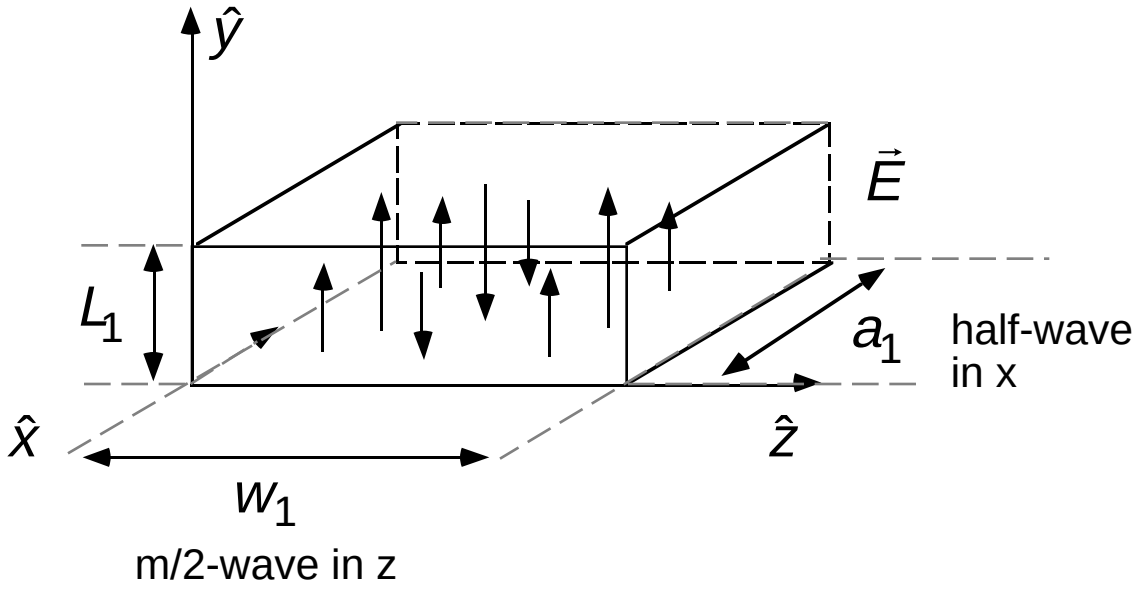

Fig. 5 A closed rectangular pillbox, excited in the TE_{10m} mode.

Adopting a phasor notation,

$$\vec{E}(\vec{r},t)=\Re\left\{\tilde{E}(\vec{r})e^{j\omega t}\right\},\ \vec{H}(\vec{r},t)=\Re\left\{\tilde{H}(\vec{r})e^{j\omega t}\right\}.$$

The TE_{10m} mode field components may be expressed as,

$$\tilde{E}_y=\tilde{E}_0\sin(\beta_x x)\sin(\beta_z z),$$
$$Z_0\tilde{H}_x=-j\frac{\beta_z}{\beta_0}\tilde{E}_0\sin(\beta_x x)\cos(\beta_z z),\quad Z_0\tilde{H}_z=j\frac{\beta_x}{\beta_0}\tilde{E}_0\cos(\beta_x x)\sin(\beta_z z).$$

The wavenumbers and resonant frequency are

$$\beta_x=\frac{\pi}{a_1},\qquad \beta_z=\frac{m\pi}{w_1},\qquad \beta_0=\frac{\omega_0}{c}=\sqrt{\beta_x^2+\beta_z^2}=\frac{\pi}{a_1}\sqrt{1+\frac{m^2a_1^2}{w_1^2}}.$$

The wall Q may be computed from

$$\frac{1}{Q_w}=\frac{\delta}{2}\frac{\int_{wall}dS\left|\tilde{H}\right|^2}{\int_{volume}dV\left|\tilde{H}\right|^2},$$

with δ the skin-depth,

$$\delta = \sqrt{\frac{2}{\mu\sigma\omega}} \approx 0.22\mu m,$$

for room-termperature copper at 91.39GHz. The result is

$$\frac{1}{Q_w} = \frac{R_s}{Z_0}\frac{2}{\beta_0}\left\{\frac{1}{L_1} + \frac{2}{w_1}\frac{\beta_z^2}{\beta_0^2} + \frac{2}{a_1}\frac{\beta_x^2}{\beta_0^2}\right\},$$

with Z_0˜376.7Ω and

$$R_s = \frac{1}{\sigma\delta} \approx 79m\Omega\ ,$$

This result may be expressed in terms of the angle $\theta_1 = \beta_0 L_1$ as

$$\frac{1}{Q_w} = 2\frac{R_s}{Z_0}\left\{\frac{1}{\theta} + \frac{2}{\pi}\frac{\left(1+\frac{m^2a_1^3}{w_1^3}\right)}{\left(1+\frac{m^2a_1^2}{w_1^2}\right)^{3/2}}\right\}.$$

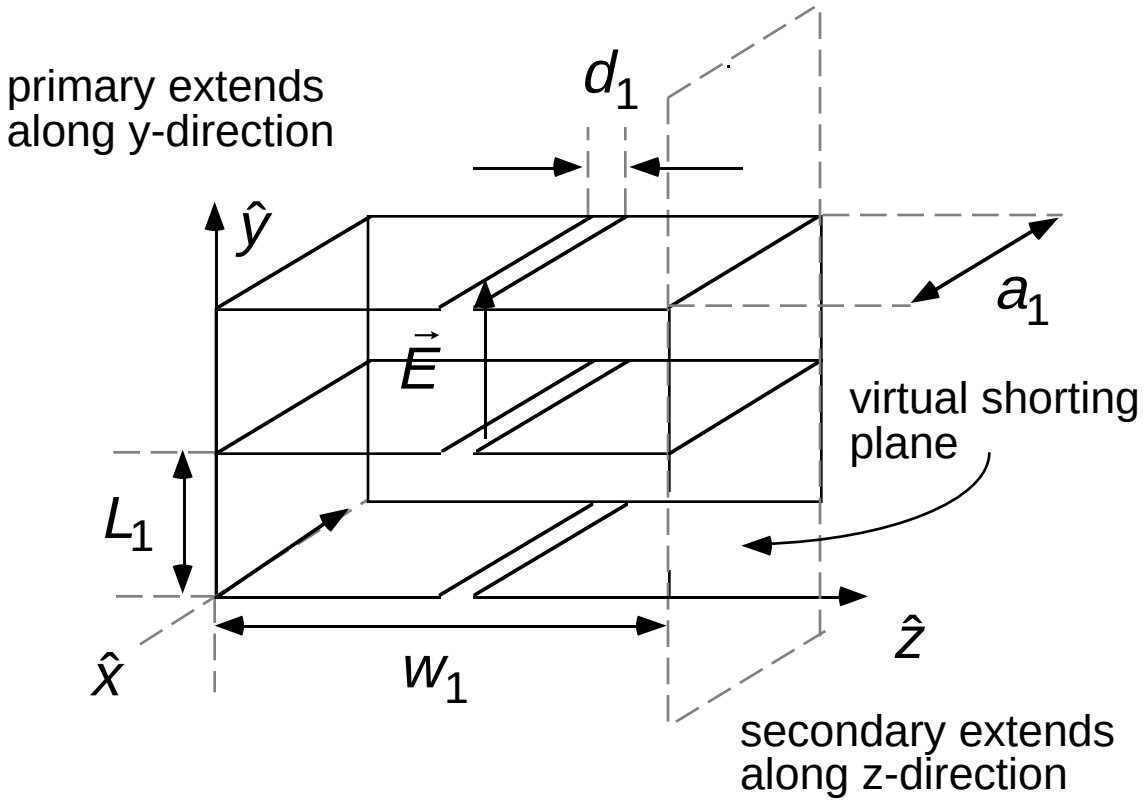

Fig. 6 The primary line consists of rectangular pillboxes coupled by apertures of width d_1 and depth a_1 equal to that of the cavities. The apertures are centered in the "broad-walls" of the cavities.

It will eventually be helpful to have the time-average Poynting flux into the walls, at the location of maximum dissipated power density on the walls, and this is,

$$S_{\max} = \frac{\omega U_1}{V_1}\eta\delta \ ,$$

where $V_1 = L_1 a_1 w_1$ is the cavity volume, and

$$\eta = 2 \times \max\begin{cases} 1 - \frac{\beta_x^2}{\beta_0^2} \\ \frac{\beta_x^2}{\beta_0^2} \end{cases} .$$

Note that $\eta \geq 1$, with equality if $ma_1 = w_1$.

Before moving on, we include mention of the problem illustrated in Fig. 6, concerning the detailed geometry required for coupling primary cells.

1.3 Requirements on the Secondary Line

Energy conservation corresponds to

$$P_1 = \frac{U_1}{L_1} V_{g1},$$

relating peak power available during charge-up of the primary, to energy U_1 stored per period length L_1 in the primary. The group velocity in the primary is V_{g1}. For subsequent analysis we will make the approximation that after switch closure adjacent cavities of the primary are uncoupled. Thus if Q_e is the external Q of a primary cavity after switch closure, then we assume that the power dumped down the secondary transmission line,

$$P_2 = \frac{\omega U_1}{Q_e} = \frac{U_2}{L_2} V_{g2},$$

is much larger than the power P_1 incident prior to switch closure. In this expression we have equated power dumped from the primary cavity to the power flowing down the transmission line, expressed in terms of energy U_2 stored per period length L_2 in the secondary. The group velocity in the secondary is V_{g2} These relations permit us to express the stored energy per cell in the secondary in terms of the power previously incident on the primary,

$$U_2 = \frac{L_2}{V_{g2}} \frac{\omega}{Q_e} \frac{L_1}{V_{g1}} P_1.$$

To determine the accelerating voltage we need the R-over-Q for one cavity of the secondary line,

$$\left[\frac{R}{Q}\right] = \frac{V_{nl}^2}{\omega U_2},$$

and this will be computed from geometric considerations in the next section. Here V_{nl} is the no-load gap voltage for a single cavity of the secondary line. Notice that the effective

unloaded accelerating gradient can be determined from

$$G_{nl} = \frac{V_{nl}}{L_1} = \frac{1}{L_1}\left\{\left[\frac{R}{Q}\right]\omega U_2\right\}^{1/2} = \left\{\frac{L_2}{L_1}\frac{1}{Q_e}\left[\frac{R}{Q}\right]\frac{\omega}{V_{g2}}\frac{\omega}{V_{g1}}P_1\right\}^{1/2}.$$

These scalings permit us to determine requirements on the basic line parameters; however they must be augmented by three additional features discussed in the following sections: achievable *[R/Q]* (Sec. 1.4), pulsed heating (Sec. 1.5), and the effect of dispersion in the secondary insofar as this sets a lower bound on the pulse length discharged into the secondary (Sec 2).

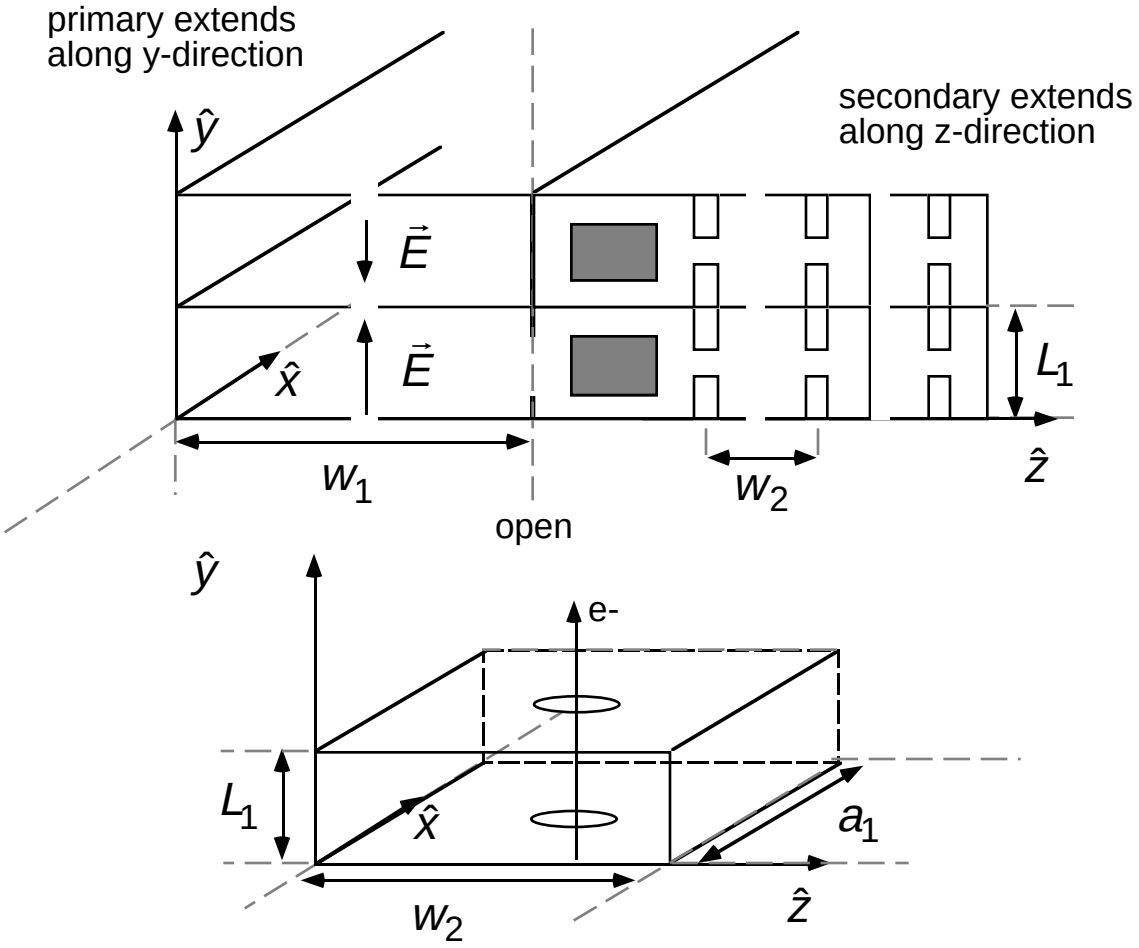

Fig. 7 Secondary transmission line, viewed as a chain of accelerating cavities.

1.4 *[R/Q]* for the Secondary Line

To compute the *[R/Q]* for the secondary transmission line viewed as an accelerator, we consider the geometry sketched in Fig. 7. Consider a particle passing through the cavity on a ballistic trajectory, aligned to the waveguide "*y*" axis. The electric field witnessed by the particle is

$$\vec{E} = \hat{y}\,\Re\tilde{E}_0 \sin(\beta_x x)\sin(\beta_z z)e^{j\omega t}.$$

and this may be integrated across the gap to obtain the energy change,

$$\Delta\varepsilon = \int_0^{L_1} dy E_y\left(x, y, z, t = t_0 + \frac{y}{c}\right),$$

expressed in terms of a cavity voltage, V_c,

$$\Delta\varepsilon = \Re\left\{\tilde{V}_c(x,z)e^{j\omega t}\right\},$$

and arrival time at the cavity entrance, t_0. The cavity voltage on the beam axis is

$$\tilde{V}_c = \tilde{E}_0 L_1 T e^{j\theta/2},$$

where θ is the transit angle,

$$\theta = \frac{\omega L_1}{c},$$

and T is the transit time factor

$$T = \frac{\sin\left(\frac{\theta}{2}\right)}{\left(\frac{\theta}{2}\right)}.$$

The stored energy may be expressed as

$$U = \frac{V}{8cZ_0}\left|\tilde{E}_0\right|^2,$$

where $V=a_2 w_2 L_1$ is the cavity volume. Thus the *R-over-Q* is

$$\left[\frac{R}{Q}\right] = \frac{\left|\tilde{V}_c\right|^2}{\omega U} = Z_0 \frac{16}{\beta_0^2 a_2 w_2}\frac{\sin^2\left(\frac{\theta}{2}\right)}{\left(\frac{\theta}{2}\right)}.$$

Optimum occurs for θ=133.56°, and corresponds to $L_1=0.37099\lambda$, and

$$\left[\frac{R}{Q}\right] = \frac{442.5\Omega}{\left[\frac{w_2}{a_2} + \frac{m^2 a_2}{w_2}\right]}.$$

Optimum shunt impedance occurs for $w_2 = m a_2$, and m=1, and corresponds to $[R/Q]$=221.3Ω, the same as that of a right cylindrical pillbox with the same transit angle. (In practice, addition of beam ports will reduce this figure and we will premise the working examples discussed below on the value $[R/Q]$=176Ω.) This choice of transit angle corresponds to $\beta_0 = \sqrt{2}\pi / a_2$, or

$$a_2 = w_2 = \frac{\lambda}{\sqrt{2}},$$

so that a_2=w_2=0.23195cm, L_1=0.121696cm and Q_w~2700. This value for Q_w assumes a surface smooth on the scale of the skin depth δ~9μinch. The loss-factor is determined from *[R/Q]* according to

$$k_l = \frac{1}{4}\omega\left[\frac{R}{Q}\right],$$

and corresponds to 32V/pC for the ideal case. Single-bunch beam-induced voltage is then $V_b \approx -2k_l Q_b$, for a charge Q_b.

1.5 Pulsed Heating

As a figure of merit for pulsed heating, we make note of the pulsed temperature rise at a "hot-spot" on the surface, corresponding to S_{max}, subject to dissipation constant in time ("square pulse"),

$$\Delta T_{\max}(t) = \frac{2S_{\max}}{\sqrt{\pi\kappa C}}t^{1/2},$$

where, for room-temperature copper,

$$\kappa = 401\frac{W}{^\circ K - m}, \qquad C = 3.45\times 10^6 \frac{J}{^\circ K - m^3}.$$

As discussed in numerous notes, the ultimate limit on this temperature rise is an ongoing and vital research problem.The value is somewhere between 40°C and the melting point of copper, 1356.5°K. Meanwhile, we simply maintain an interest in keeping the pulsed temperature rise as low as possible, in applying the following analysis; examples discussed below are premised, quite arbitrarily, on 152°K.

Making use of our calculation of cavity voltage, we may express the maximum average Poynting flux into the copper as

$$S_{\max} = \frac{1}{8}\frac{G^2\delta\beta_0}{Z_0 T^2}\eta,$$

where T is the transit time factor, and recall $\eta \geq 1$, with η=1 for a_2=w_2.

1.6 Example of Design Considerations

At this point there is still one more design consideration to cover, and that is the choice of group velocity. Inputs to this choice are: the effect of dispersion (to be quantified in the section following) and losses & power requirements. However, it is helpful to pause at this point to illustrate the scalings set down thus far. The following discussion will serve to motivate the detailed analysis of dispersion that follows in Sec. 2. We proceed to set down some parameters for a matrix linac.

We suppose an *[R/Q]* of 176Ω, corresponding to a loss factor of 25.3V/pC. To compute the stored energy required in one secondary cell, we employ

$$U_2 = \frac{V_{NL}^2}{4k_l},$$

and at this point we realize we must choose the transit angle (identical to the phase-advance per cell in the primary). We assume a transit angle of 133.56°, as one can show that this minimizes the requirement on stored energy per unit length in the primary. The gap length, L_1, is then 1.2210^{-3}m. To insure a minimum loaded gradient of 1.01GV/m for the N=50 (last) bunch, and at 60pC per bunch, we should operate with an unloaded gradient of 1.13GV/m. The no-load voltage corresponding to a 1.13GV/m accelerating field is 1.4MV. This voltage appears in a cell when the energy in the cell reaches U_2=19mJ.

At this point we have enough information to compute the pulsed temperature rise in terms of the (as yet undecided) exposure time of the copper in the secondary. The Poynting flux is

$$S = \frac{1}{8}\frac{G^2\beta_0\delta}{Z_0 T^2}\eta,$$

with δ=0.22μm, β_0=1.9x10^{3}m^{-1}, and transit angle factor T˜0.789. Taking $a_2=w_2$ (corresponding to minimum η), the peak dissipation on the walls is 2.89x10^{11}W/m^2, and the pulsed temperature rise

$$\Delta T = 3.03\times 10^{-5}\,^\circ K\, S\left(\mathrm{W/m^2}\right) t^{1/2}(\mathrm{sec})$$

is 279°K for a 1ns exposure. This is the point in the design at which maximum acceptable pulsed temperature rise enters. Absent this information, we must make a choice as to exposure time, realizing that dispersion will set a lower bound. For a 0.3ns exposure time, the pulsed temperature rise is 152°K (119°K at the 1GeV/m end of the secondary). For the purposes of definiteness, we will take this value of 152°K as the pulsed temperature limit, and constrain other parameters accordingly. Thus we decide to work with

$$T_p = 0.3ns = 27.5 \text{ rf cycles} \quad \Leftrightarrow \quad \Delta T = 152\,^\circ K.$$

The implication for the primary is that a primary cell should then discharge in 27.5 rf cycles (one rf cycle is 10.9ps at 91.39GHz), and thus would be no more than 14 wavelengths in width, and if much less, would have been designed to disharge as a cavity with an output waveform that approaches an exponential in the limit of a small cavity.

Next we need to choose the initial group velocity for the secondary line, realizing that there is a minimum set by losses and the required length of the line (N=50 periods). More significantly, too low a value will result in untenable dispersion---*i.e.*, too low an initial group velocity would be inconsistent with the presumed pulse length of 0.3ns. Meanwhile, too high a value would require excessive peak power discharged into the line, and consequently, excessive stored energy in the primary line. To inform our choice of group velocity, let us recall the scalings for a quasiperiodic line with constant stored energy per cell---just the constant gradient structure scalings in a different venue. Group velocity varies linearly along the secondary line

$$V_g(z) = V_g(0) - \frac{\omega_0}{Q_w}z,$$

and the initial group velocity is related to the attenuation parameter, τ,

$$V_g(0) = \frac{\omega_0 L_s}{Q_w}\left(1 - e^{-2\tau}\right)^{-1},$$

defined for the steady-state problem, in terms of power incident on the secondary, $P(0)$, with respect to the power to the load at the end of the secondary, $P(L_s)$,

$$e^{-2\tau} = \frac{P(L_s)}{P(0)} = \frac{V_g(L_s)}{V_g(0)}.$$

Secondary wall Q has already been determined by our choice of cell dimensions, and is 2700. This sets the natural field decrement time to

$$T_0 = \frac{2Q_w}{\omega_0} \approx 9.4ns.$$

The value for wall Q, and the choice of structure length $L_s = 2^{-1/2} N\lambda \approx 11.6cm$ set the minimum initial group velocity,

$$\min \frac{V_g(0)}{c} = \frac{\omega_0 L_s}{cQ_w} = 2^{1/2}\pi \frac{N}{Q_w} \approx 0.082.$$

However, we will need to stay far from this value to avoid dispersion loss of peaking voltage near the end of the secondary. Let us consider a couple of example choices of initial group velocity, and the consequences.

Example 1 --- "High" Group Velocity

We suppose $V_{g2} \equiv V_g(0) = 0.23c$. Peak power switched into the secondary is then $P_2 = U_2 V_{g2} / L_2 \approx 5.6 \times 10^2 MW$. The attenuation parameter,

$$\tau = -\frac{1}{2}\ln\left(1 - 2\frac{L_s}{V_g(0)T_0}\right) \approx 0.221,$$

The fill time,

$$T_f = \int_0^{L_s} \frac{dz}{V_g} = -\frac{Q_w}{\omega_0}\ln\left(1 - \frac{\omega_0 L_s}{Q_w V_g(0)}\right) = \frac{2Q_w}{\omega_0}\tau \approx 2.08ns;$$

although, it should be emphasized that the structure doesn't fill; this quantity is the time for the rf pulse to make its way through the secondary. This sets the separation in time of the first and last bunch. Final group velocity is $V_g(L_s) = 0.148c$. The energy that must be stored in the primary cell prior to switch opening is

$$U_1 \approx P_2 T_p = \frac{U_2 V_{g2} T_p}{L_2} \approx 0.168J,$$

and we use an approximate equality since, in the case of a primary cell discharging as a cavity (rather than a transmission line), losses to the walls would impose a correction. The energy density stored in the primary line is then

$$u_1 = \frac{U_1}{L_1} = 138 J/m.$$

Let us underscore the interest in this number. We would like to build a 1 GeV linac, and it should be compact, not crowded with tubes and modulators. For example, one 50MW tube with a 1 μs pulse will provide on the order of 20J, after losses in compression.[1] Thus a requirement of 100J/m amounts to a requirement of five 50MW tubes for a 1 GeV linac. In terms of footprint, one has a table with a 3.3 feet long, 5-inch wide strip of copper, being fed by five SLAC modulators. This strikes one as quite enough in the way of modulators. The more elaborate version of this concern has to do with site-power for a high-energy collider, in the face of realistic efficiencies for the rf complex. We will be providing 50 x 60pC x 1GeV/m = 3J/m to the beam. Let us suppose we expend 50J/m in the primaries, and, let us say, 125J/m from the tubes. This corresponds to a 2.4% efficiency of transfer of rf from the tube output to beam kinetic energy. Let us suppose that the product of additional efficiencies comes to the optimistic figure of 20%---including, efficiency of conversion of wall-plug power to tube-beam power, efficiency of conversion of tube-beam power to rf pulse power, and any other losses . Then net efficiency is 0.5%. The implication is then that for a collider, with a total of 6nC at 2.5 TeV, running at 120Hz, the average beam power would be 1.8MW, and the site power load due to the rf system would be 360MW. Now the criterion for acceptable site-power for a collider lies beyoned the realm of physics scalings, and is not well-defined. We must have a working figure, however; we will suppose, aribtrarily that 500MW is a firm upper value, and 360MW is a desireable value. In this case, our "Example 1" choice of group velocity is not tenable as it corresponds to a site-power of 812MW (and that is before accounting for magnet power supplies and sundries). Evidently, we would prefer $u_1 \approx 50 J/m$, or as close as we can get to that figure. This motivates a second example.

Example 2 --- "Medium" Group Velocity

For $V_{g2} \equiv V_g(0) = 0.174c$, $V_g(L_s) = 0.092c$, and $u_1 = 105 J/m$, corresponding to a 5-tube 1-GeV-linac (in the sense of the foregoing discussion) and a 620 MW collider. This example will prove to be quite close to the limit due to dispersion.

Example 3 --- "Low" Group Velocity

We suppose $V_{g2} \equiv V_g(0) = 0.15c$. This is "low" in the sense that $V_g(L_s) = 0.0677c$, and, as we will see, it proves challenging to maintain transient peaking voltage in such a device. For this case $u_1 = 90 J/m$, corresponding to a 5-tube 1-GeV-linac (in the sense of the foregoing discussion) and a 540MW collider. Attenuation parameter is $\tau \approx 0.40$, fill-time is $T_f = 3.7 ns$. From the system point of view, not yet having glimpsed the effect of dispersion, this looks promising.

Appreciating the need for low group velocity, on the order of $V_{g2} \equiv V_g(0) = 0.15c$, and short pulse length, $T_p = 0.3 ns = 27.5 \text{ rf cycles}$, let us consider in detail the fundamental conflict between these two requirements: dispersion. Maxwell's equations imply a fundamental relation between bandwidth and steady-state energy-storage. In the face of this, we seek next to quantify how short a pulse we may propagate in a transmission line with low group velocity (*i.e.*, one that is good at storing energy). The two features of the problem that bear in our favor are: (1) a peaking voltage is required in a secondary cell for only a short duration, *i.e.*, we are not interested in filling the structure (2) the transmission characteristics (dispersion curve) for the secondary may be designed without the usual synchronism constraint that applies to conventional travelling wave

structure. We must exploit these features.

2. Wave Propagation & Dispersion on the Secondary Line

To quantify dispersion in the secondary, we may proceed analytically, or simply employ a numerical coupled cavity model. To guide our thinking, let us formulate an analytic model first for the case of a uniform line. We can then test our results on the more realistic tapered line.

2.1 Analytic Formulation

We consider a uniform transmission line characterized by a dispersion relation $\beta(\omega)$, specifying wavenumber as a function of angular frequency. We will make use of two alternative notations: one for phase advance per period $\theta(\omega) = \beta(\omega)L_2$, where L_2 is the period length, and one for phase-advance between 0 and a point z $\Theta(\omega, z) = \beta(\omega)z$. We suppose that a voltage is specified at the input to the line (z=0), as the real part of

$$V(t,0) = \tilde{V}_0(t)e^{j\omega_0 t},$$

The phasor $\tilde{V}_0(t)$ conveys both amplitude and frequency modulation information. In the frequency domain we have,

$$\tilde{V}(\omega,0) = \int_{-\infty}^{\infty} \frac{dt}{\sqrt{2\pi}} \tilde{V}_0(t)e^{j(\omega_0-\omega)t},$$

and the modulation may be expressed as

$$\tilde{V}_0(t) = \int_{-\infty}^{\infty} \frac{d\omega}{\sqrt{2\pi}} \tilde{V}(\omega,0)e^{j(\omega-\omega_0)t}.$$

We may compute the voltage at a location z, by evaluating the integral,

$$\begin{aligned} V(t,z) &= \int_{-\infty}^{\infty} \frac{d\omega}{\sqrt{2\pi}} \tilde{V}(\omega,0)e^{j\omega t - j\beta(\omega)z} \\ &= e^{j\omega_0 t - j\beta(\omega_0)z} \int_{-\infty}^{\infty} \frac{d\omega_1}{\sqrt{2\pi}} \tilde{V}(\omega_0+\omega_1,0)e^{j\omega_1 t - j[\beta(\omega)-\beta(\omega_0)]z}, \\ &= e^{j\omega_0 t - j\beta(\omega_0)z}\tilde{V}_z \end{aligned}$$

where

$$\tilde{V}_z = \int_{-\infty}^{\infty} \frac{d\omega_1}{\sqrt{2\pi}} \tilde{V}(\omega_0+\omega_1,0)e^{j\Phi},$$

and

$$\begin{aligned} \Phi &= \omega_1 t - \left[\beta(\omega) - \beta(\omega_0)\right]z \\ &= \omega_1 t - z\left[\beta'(\omega_0)\omega_1 + \frac{1}{2!}\beta''(\omega_0)\omega_1^2 + \frac{1}{3!}\beta'''(\omega_0)\omega_1^3 + \ldots\right]. \end{aligned}$$

We introduce the variable,

$$\tau = t - z\beta'(\omega_0),$$

in terms of which we have

$$\Phi = \Phi(\omega_1, \tau, z) = \omega_1\tau - z\left[\frac{1}{2}\beta''(\omega_0)\omega_1^2 + \frac{1}{6}\beta'''(\omega_0)\omega_1^3 + \ldots\right],$$

and,

$$\begin{aligned}\tilde{V}_z(\tau) &= \int_{-\infty}^{\infty}\frac{d\omega_1}{\sqrt{2\pi}}\tilde{V}(\omega_0+\omega_1,0)\exp\{j\Phi(\omega_1,\tau,z)\} \\ &= \int_{-\infty}^{\infty}\frac{d\omega_1}{\sqrt{2\pi}}\tilde{V}(\omega_0+\omega_1,0)\exp\left\{j\omega_1\tau - jz\left[\frac{1}{2}\beta''(\omega_0)\omega_1^2 + \frac{1}{6}\beta'''(\omega_0)\omega_1^3 + \ldots\right]\right\}.\end{aligned}$$

Note that when dispersion is negligible (second and higher derivatives of wavenumber are small), we have $\tilde{V}_z(\tau) = \tilde{V}_0(\tau)$ and we recover the familiar result,

$$V(t,z) \approx e^{j\omega_0\left(t - z/V_\varphi\right)}\tilde{V}_0\left(t - z/V_g\right),$$

where the constant phase-fronts travel at

$$V_\varphi = \frac{\omega}{\beta} = \text{phase} - \text{velocity}$$

while any modulation ("information") in $\tilde{V}_0$ travels at

$$V_g = \frac{1}{\beta'(\omega_0)} = \text{group} - \text{velocity}.$$

Our interest is in evaluating this integral for representative waveforms in the presence of dispersion. Let us make use of

$$\tilde{V}(\omega_0+\omega_1,0) = \int_{-\infty}^{\infty}\frac{d\tau'}{\sqrt{2\pi}}\tilde{V}_0(\tau')e^{-j\omega_1\tau'},$$

to express the downstream voltage,

$$\begin{aligned}\tilde{V}_z(\tau) &= \int_{-\infty}^{\infty}\frac{d\omega_1}{\sqrt{2\pi}}\int_{-\infty}^{\infty}\frac{d\tau'}{\sqrt{2\pi}}\tilde{V}_0(\tau')e^{-j\omega_1\tau'}\exp\{j\Phi(\omega_1,\tau,z)\} \\ &= \int_{-\infty}^{\infty}d\tau'\,\tilde{V}_0(\tau')\frac{1}{2\pi}\int_{-\infty}^{\infty}d\omega_1\exp\{j\Phi(\omega_1,\tau-\tau',z)\}, \\ &= \int_{-\infty}^{\infty}d\tau'\,\tilde{V}_0(\tau')G(\tau-\tau',z)\end{aligned}$$

in terms of the propagator,

$$G(\tau,z)=\frac{1}{2\pi}\int_{-\infty}^{\infty}d\omega_1\exp\{j\Phi(\omega_1,\tau,z)\}$$
$$=\frac{1}{2\pi}\int_{-\infty}^{\infty}d\omega_1\exp\left\{j\omega_1\tau-jz\left[\frac{1}{2}\beta''(\omega_0)\omega_1^2+\frac{1}{6}\beta'''(\omega_0)\omega_1^3+\ldots\right]\right\}.$$

In the absence of dispersion $G(\tau,z)=\delta(\tau)$. Let us evaluate *G* for two representative cases. In tinkering with the integral, it is helpful to note the equivalent expression in terms of a contour integral, in the complex plane,

$$G(\tau,z)=\frac{1}{2\pi j}\int_{-j\infty+}^{j\infty+}dp\exp\{j\Phi(-jp,\tau,z)\},$$

where the "+" sign in the limits reminds us that the contour is taken to the right of all poles in the integrand, consistent with causality. Note that

$$\Phi(-jp,\tau,z)=p\tau+\frac{j}{2}(z\beta'')p^2-\frac{1}{6}(z\beta''')p^3+\ldots=p\tau+\frac{j}{2}\Theta''p^2+\frac{1}{6}\Theta'''p^3+\ldots,$$

where $\Theta(\omega,z)=\beta(\omega)z$ is the cumulative phase-advance, and the derivatives with respect to frequency are evaluated at $\omega=\omega_0$.

In the limit that first-order dispersion dominates transmission (β''' and higher derivatives vanish), we have

$$G\approx\frac{1}{2\pi j}\int_{-j\infty+}^{j\infty+}dp\exp\left\{p\tau+\frac{j}{2}\Theta''p^2\right\}=\frac{1}{\sqrt{2\pi\, j\Theta''}}\exp\left\{\frac{j\tau^2}{2\Theta''}\right\},\quad \textit{(1st Order Dispersion)}$$

where we rotated the contour to reduce the problem to the integral of a Gaussian. If, on the other hand, the transmission line is designed for zero first-order dispersion,

$$\beta''(\omega_0)=0,$$

and neglecting third and high-order terms, we have

$$G\approx\frac{1}{2\pi j}\int_{-j\infty+}^{j\infty+}dp\exp\left\{p\tau+\frac{1}{6}\Theta'''p^3\right\}$$
$$=\int_0^{\infty}d\omega_1\cos\left\{\frac{1}{6}\Theta'''\omega_1^3-\omega_1\tau\right\}\quad,\qquad\textit{(2nd Order Dispersion)}$$
$$=\left(\frac{2}{\Theta'''}\right)^{1/3}Ai\left(-\left(\frac{2}{\Theta'''}\right)^{1/3}\tau\right)$$

with *Ai* the Airy function.

Distortion of a "Top-Hat" Pulse

Let us next apply our results to a specific waveform, a "top-hat",

$$\tilde{V}_0(t) = H(t)H\left(T_p - t\right) = \begin{cases} 0\,; t < 0 \\ 1\,; 0 < t < T_p \\ 0\,; T_p < t \end{cases},$$

with H the step-function. This corresponds to

$$\tilde{V}(\omega_0 + \omega_1, 0) = \int_{-\infty}^{\infty} \frac{d\tau'}{\sqrt{2\pi}} \tilde{V}_0(\tau') e^{-j\omega_1 \tau'} = \int_0^{T_p} \frac{d\tau'}{\sqrt{2\pi}} e^{-j\omega_1 \tau'} = \frac{1}{\sqrt{2\pi}} \frac{1 - e^{-j\omega_1 T_p}}{j\omega_1}.$$

The downstream voltage phasor is just

$$\tilde{V}_z(\tau) = \int_0^{T_p} d\tau' \, G(\tau - \tau', z).$$

In the case where first-order dispersion dominates, this integral becomes

$$\tilde{V}_z(\tau) = \int_0^{T_p} d\tau' \frac{1}{\sqrt{2\pi \, j\Theta''}} \exp\left\{ \frac{j(\tau - \tau')^2}{2\Theta''} \right\}$$

we introduce the notation $\Theta'' = \sigma \left| \Theta'' \right|$, with $\sigma = \pm 1$, the normalization,

$$\hat{\tau} = \frac{\tau}{\sqrt{\pi \left| \Theta'' \right|}}, \quad \hat{T}_p = \frac{T_p}{\sqrt{\pi \left| \Theta'' \right|}},$$

and the Fresnel integrals,

$$C(x) = \int_0^x \cos\left(\frac{\pi}{2} t^2 \right) dt, \qquad S(x) = \int_0^x \sin\left(\frac{\pi}{2} t^2 \right) dt,$$

and $E = C + j\sigma S$.

In terms of Fresnel integrals,

$$\tilde{V}_z(\tau) = \frac{1}{\sqrt{2\,j}} \int_0^{\hat{T}_p} d\hat{\tau}' \exp\left[j \frac{\pi}{2} \sigma \left(\hat{\tau} - \hat{\tau}' \right)^2 \right]$$

$$= \frac{1}{\sqrt{2\,j}} \int_{-\hat{\tau}}^{\hat{T}_p - \hat{\tau}} d\hat{\tau}' \exp\left[j \frac{\pi}{2} \sigma \hat{\tau}'^2 \right] = \frac{1}{\sqrt{2\,j}} \left\{ E\left(\hat{T}_p - \hat{\tau} \right) + E\left(\hat{\tau} \right) \right\}.$$

Some properties of the Fresnel integrals are helpful at this point. They are odd $E(z) = -E(-z)$. For small arguments,

$$C(z) \approx z - \frac{\pi^2}{40} z^5, \qquad S(z) \approx \frac{\pi}{6} z^3 - \frac{\pi^3}{336} z^7 .$$

For large arguments,

$$C(z) \approx \frac{1}{2} + \frac{1}{\pi z} \sin\left(\frac{\pi}{2} z^2\right) - \frac{1}{\pi^2 z^3} \cos\left(\frac{\pi}{2} z^2\right),$$
$$S(z) \approx \frac{1}{2} - \frac{1}{\pi z} \cos\left(\frac{\pi}{2} z^2\right) - \frac{1}{\pi^2 z^3} \sin\left(\frac{\pi}{2} z^2\right).$$

and asymptotically,

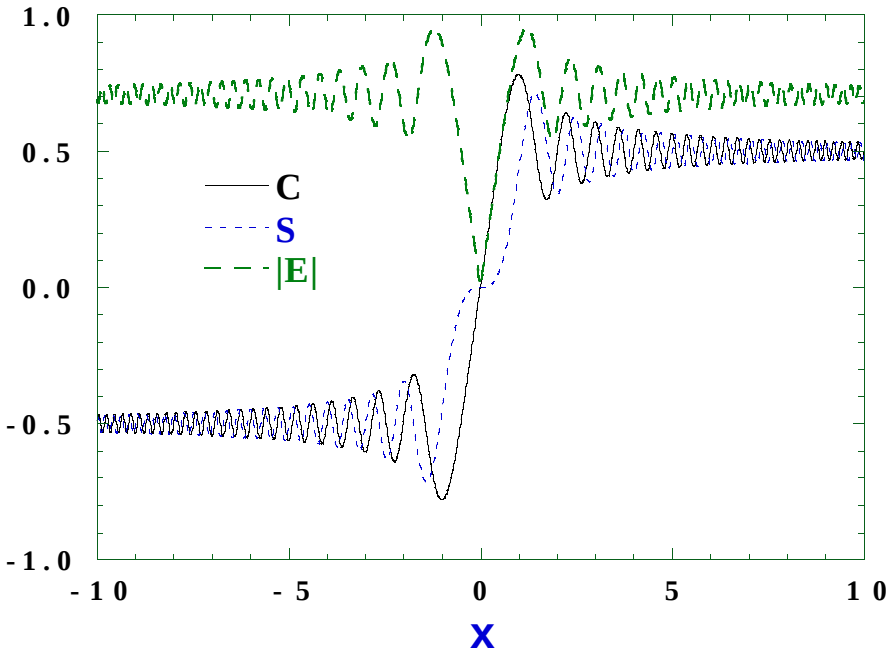

Fig. 8 Fresnel integrals.

$$\lim_{z \to \infty} E(z) = \sqrt{\frac{j}{2}} .$$

For a short pulse, $\hat{T}_p << 1$, one has

$$\tilde{V}_z(\tau) \approx \frac{\hat{T}_p}{\sqrt{2\,j}} e^{j\frac{\pi}{2}\sigma\hat{\tau}^2} \quad ,$$

and for a long pulse it is easy to see that $\tilde{V}_z(\tau) \approx 1$ in the interior of the pulse. More detailed quantitative progress is aided by the routine in *Numerical Recipes* for calculation of the Fresnel integrals. Figure 9 illustrates the waveforms for several values of pulse length.

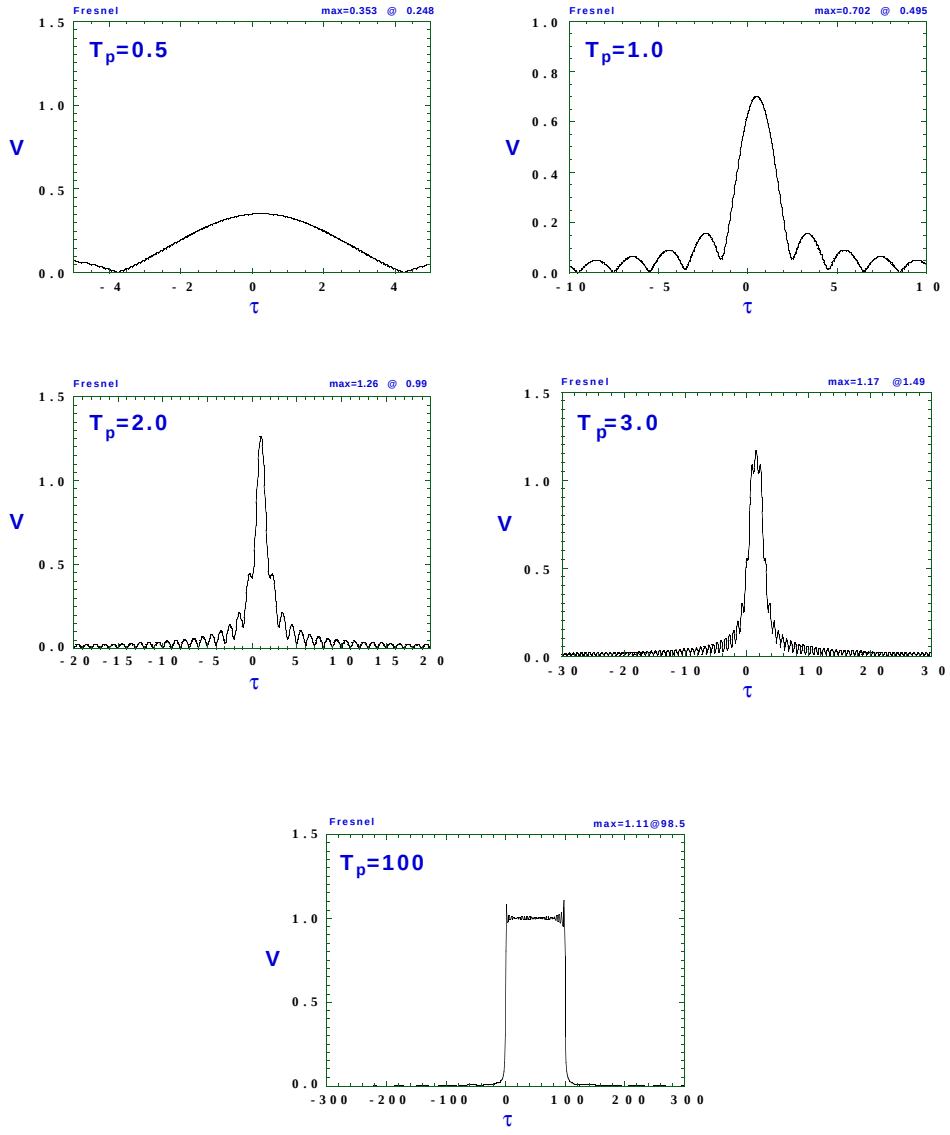

Fig. 9 Depicted are voltage waveforms versus normalized time, for an initially square pulse of unit amplitude, after first-order dispersion in a periodic line, for several values of normalized pulse length.

Inspecting these plots, one can see that a voltage waveform, travelling down the line develops a peaking voltage larger than unity, and then broadens. To employ such a waveform for acceleration, one must know, at each z, the voltage a bunch will witness if it passes at time t, and then, the appropriate choice of t. At a fixed location z, real time is

$$t = \frac{z}{V_g} + \left(\pi|\beta''|z\right)^{1/2}\hat{\tau},$$

and the waveform shape is characterized by

$$\hat{T}_p = \frac{T_p}{\left(\pi|\beta''|z\right)^{1/2}}.$$

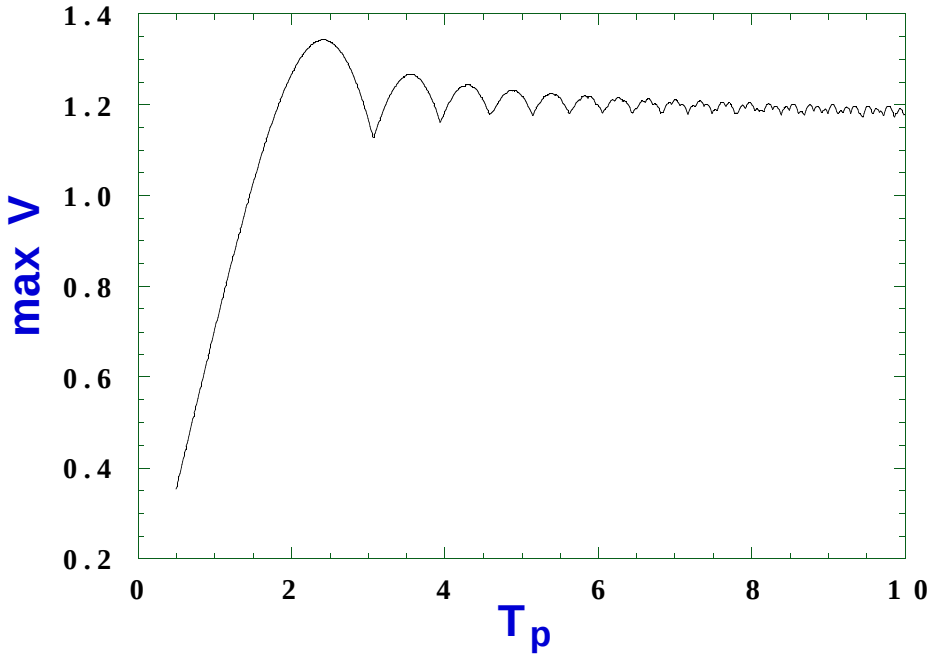

Fig. 10 Maximum peaking voltage as a function of normalized pulse length, for transport dominated by first-order dispersion.

For present purposes, we put aside the matter of the bunch schedule, which is in any case, somewhat fungible, and satisfy ourselves with a plot of maximum peaking voltage versus $\hat{T}_p$, as seen in Fig. 10. This is just the result of the survey of a few hundred of the sort of plots depicted in Fig. 9, picking out the maximum for each plot, and converting the resulting table to a plot. Inspecting this result one finds that as long as $\hat{T}_p$>1.46, the peak voltage is greater than or equal to the initial pulse length. This condition is just

$$T_p > 2.59\left(|\beta''|L_s\right)^{1/2},$$

where L_s is the required structure length.

Next let us consider the case of zero first-order dispersion; in this case the natural normalization for time is

$$\hat{\tau} = \left(\frac{2}{\Theta'''}\right)^{1/3}\tau, \qquad \hat{T}_p = \left(\frac{2}{\Theta'''}\right)^{1/3}T_p,$$

the propagator is

$$G(\tau) \approx \left(\frac{2}{\Theta'''}\right)^{1/3} Ai\left(-\left(\frac{2}{\Theta'''}\right)^{1/3}\tau\right),$$

and the downstream waveform is,

$$\tilde{V}_z(\tau) = \int_0^{T_p} d\tau' G(\tau - \tau', z) = \int_0^{\bar{T}_p} dx\, Ai\left(x - \hat{\tau}\right) = \int_{\hat{\tau}-\bar{T}_p}^{\hat{\tau}} dx\, Ai(-x).$$

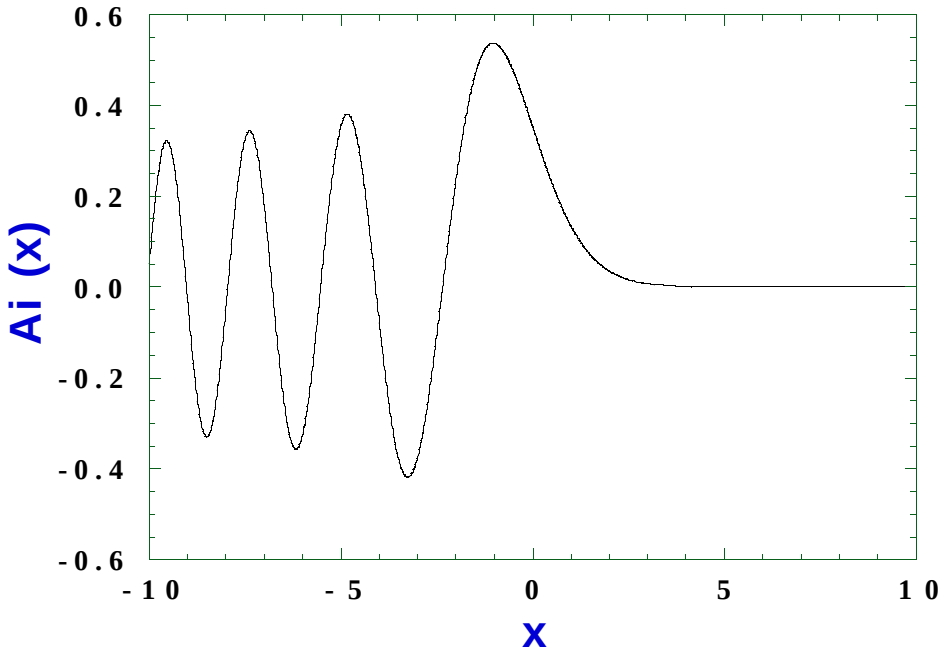

Fig. 11 The Airy function, *Ai*.

At this point, we develop an interest in the Airy function. For positive arguments the Airy function damps exponentially, for negative arguments it oscillates with algebraic diminution at large arguments. The Airy function may be expressed in terms of Bessel functions of fractional order,

$$Ai(x>0) = \left(\frac{x}{3\pi^2}\right)^{1/2} K_{1/3}(z), \qquad Ai(-x>0) = \left(\frac{x}{4}\right)^{1/2}\left\{J_{1/3}(z) - \frac{1}{3^{1/2}} Y_{1/3}(z)\right\},$$

where

$$z = \frac{2}{3}x^{3/2} \qquad \Leftrightarrow \qquad x = \left(\frac{3}{2}z\right)^{2/3}.$$

Derivatives are

$$Ai'(x>0) = -\frac{x}{\left(3\pi^2\right)^{1/2}} K_{2/3}(z), \qquad Ai'(-x>0) = \frac{x}{2}\left\{J_{2/3}(z) + \frac{1}{3^{1/2}} Y_{2/3}(z)\right\}.$$

Additional information (values, tables, plots, etc.) may be found in Abramowitz and Stegun,

$$Ai(0) = \left[3^{2/3}\Gamma\left(\tfrac{2}{3}\right)\right]^{-1} = 0.35502\ 80538\ldots, \qquad Ai'(0) = -\left[3^{1/3}\Gamma\left(\tfrac{1}{3}\right)\right]^{-1} = -0.25881\ 94037\ldots$$

The first zero of *Ai* is

$$a_1 = -2.33810\ 741\ldots, \qquad Ai'\left(a_1\right) = 0.70121\ 082\ldots$$

The first zero of Ai' is

$$a_1' = -1.01879\ 297\ldots, \qquad Ai\left(a_1'\right) = 0.53565\ 666\ldots$$

For small argument,

$$Ai(x) = Ai(0)\left\{1 + \frac{1}{6}x^3 + \frac{1}{180}x^6 + \ldots\right\} + Ai'(0)\left\{x + \frac{1}{12}x^4 + \frac{1}{504}x^7 + \ldots\right\},$$

and for large arguments,

$$Ai(x >> 1) \approx \frac{e^{-z}}{2\pi^{1/2}x^{1/4}}, \qquad Ai(-x >> 1) \approx \frac{1}{\pi^{1/2}x^{1/4}} \sin\left(z + \frac{\pi}{4}\right).$$

We will be interested in convolution integrals with the Airy function; in fact, for the top-hat pulse, our convolution integral is just the integral of the Airy function itself, and this may be expressed in terms of

$$Gi(x) = \frac{1}{\pi}\int_0^\infty dt\ \sin\left(\frac{1}{3}t^3 + xt\right),$$

as

$$\int_0^x Ai(t)\,dt = \frac{1}{3} + \pi\left\{Ai'(x)Gi(x) - Ai\,(x)Gi'(x)\right\},$$
$$\int_0^x Ai(-t)\,dt = -\frac{1}{3} + \pi\left\{Ai'(-x)Gi(-x) - Ai\,(-x)Gi'(-x)\right\}.$$

Asymptotic forms are

$$\int_0^x Ai(-t)\,dt \approx \frac{2}{3} - \frac{1}{\pi^{1/2}x^{3/4}}\cos\left(z + \frac{\pi}{4}\right), \qquad \int_{-x<0}^0 Ai(-t)\,dt \approx \frac{1}{3} - \frac{e^{-z}}{2\pi^{1/2}x^{3/4}}.$$

Roughly, 1/3 of the area integral comes from the region of positive argument, and 2/3 from the region of negative argument.

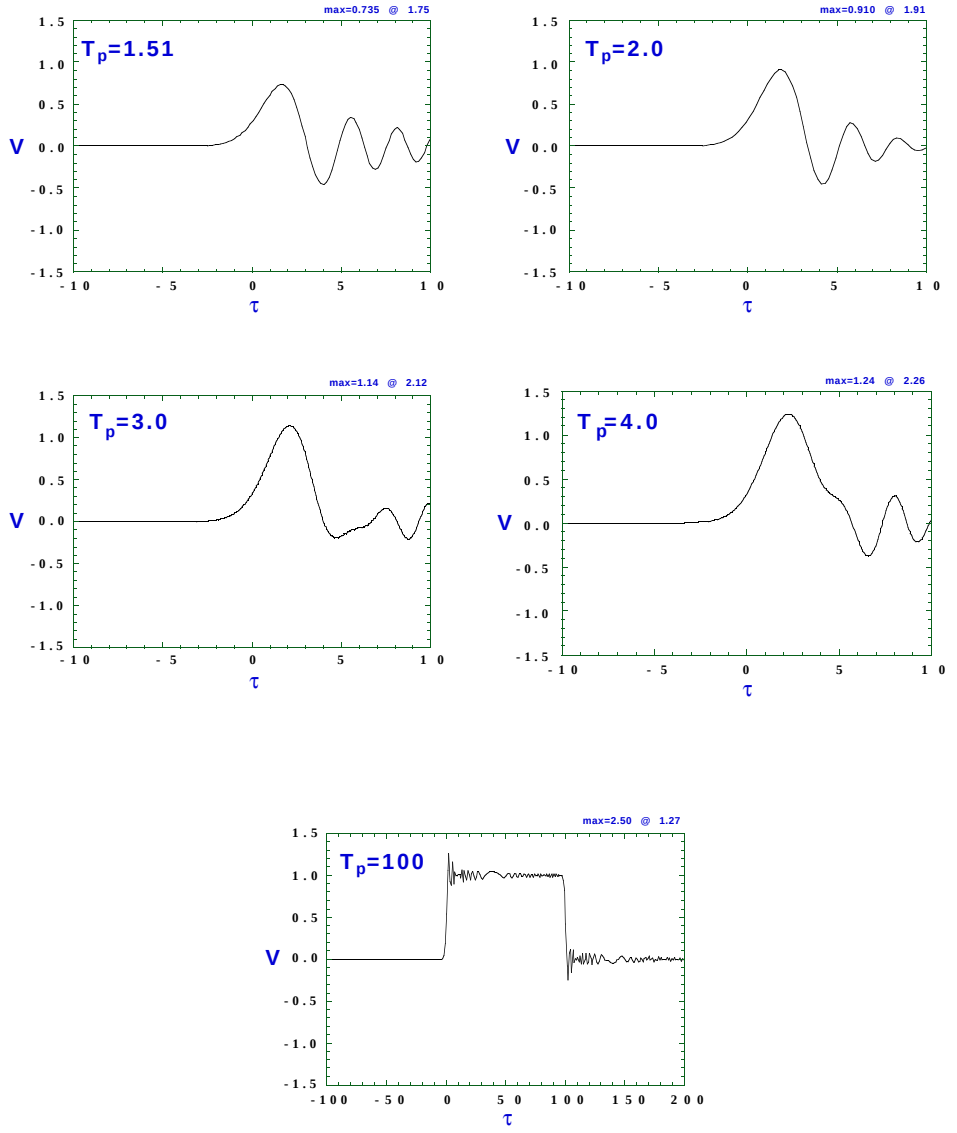

Fig. 12 Depicted are voltage waveforms versus normalized time, for an initially square pulse of unit amplitude, after second-order dispersion dominated transport in a periodic line, for several values of normalized pulse length.

In the limit of a long pulse, $\hat{T}_p >> 1$, and well after "turn-on" ($1 << \hat{\tau}$) and well before "turn-off" ($1 << \hat{T}_p - \hat{\tau}$) we may use the asymptotic integrals,

$$\int_0^{\hat{\tau}} Ai(-t)\,dt \approx \frac{2}{3} - \frac{1}{\pi^{1/2}\hat{\tau}^{3/4}}\cos\left(\frac{2}{3}\hat{\tau}^{3/2} + \frac{\pi}{4}\right), \qquad \int_{\hat{\tau}-\hat{T}_p}^{0} Ai(-t)\,dt \approx \frac{1}{3} - \frac{\exp\left(-\frac{2}{3}\left[\hat{T}_p - \hat{\tau}\right]^{3/2}\right)}{2\pi^{1/2}\left[\hat{T}_p - \hat{\tau}\right]^{3/4}},$$

to obtain

$$\tilde{V}_z(\tau) \approx 1 - \frac{\exp\left(-\frac{2}{3}\left[\hat{T}_p - \hat{\tau}\right]^{3/2}\right)}{2\pi^{1/2}\left[\hat{T}_p - \hat{\tau}\right]^{3/4}} - \frac{1}{\pi^{1/2}\hat{\tau}^{3/4}}\cos\left(\frac{2}{3}\hat{\tau}^{3/2} + \frac{\pi}{4}\right).$$

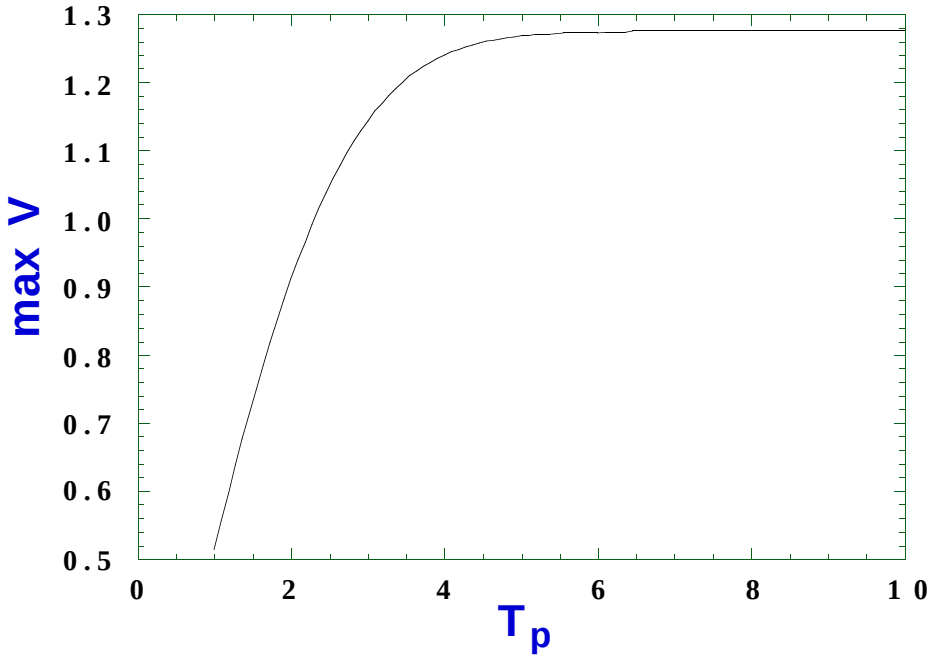

Fig. 13 Maximum peaking voltage as a function of normalized pulse length, for transport dominated by second-order dispersion.

In the case of a short pulse, $\hat{T}_p \le 1$, we have a bit more work to do. Our specific interest is the maximum in the voltage waveform downstream. This corresponds to a normalized time τ_* such that

$$0 = \frac{\partial \tilde{V}_z}{\partial \tau}(\tau_*) = \int_0^{T_p} d\tau' \frac{\partial G}{\partial \tau}(\tau - \tau', z) = G(\tau_*, z) - G(\tau_* - T_p, z).$$

(One expects the waveform to be zero at $\pm\infty$ and thus to possess at least one maximum in the interior.) Thus we are interested in roots of

$$0 = Ai(-\hat{\tau}_*) - Ai(\hat{T}_p - \hat{\tau}_*) \approx Ai'(-\hat{\tau}_*)\hat{T}_p,$$

where in the last equality we make the short pulse approximation. Thus we expect to find that

$$\tilde{V}_z\left(\tau = -\left(\frac{\Theta'''}{2}\right)^{1/3} a_1'\right) = \int_{-a_1'-\hat{T}_p}^{-a_1'} dx\, Ai(-x) \approx Ai'(a_1')\hat{T}_p,$$

is a maxmium for a short pulse. More explicitly

$$\max \tilde{V}_z \approx 0.536\left(\frac{2}{\Theta'''}\right)^{1/3} T_p, \quad \tau = 1.019\left(\frac{\Theta'''}{2}\right)^{1/3} \qquad \text{for} \qquad \hat{T}_p << 1.$$

In general we would prefer to have more precise results, as depicted in Fig. 12, together with a summary as in Fig. 13 of the maximum voltage versus normalized pulse length. One finds that for $\hat{T}_p \geq 2.3$, the maximum voltage is greater than or equal to the initial voltage amplitude. In terms of unnormalized coordinates,

$$t = \frac{z}{V_g} + \left(\frac{\beta''' z}{2}\right)^{1/3} \hat{\tau}, \qquad T_p = \left(\frac{\beta''' z}{2}\right)^{1/3} \hat{T}_p,$$

and the pulse length requirement is

$$T_p \geq 1.8\left(\beta''' z\right)^{1/3}.$$

Top-Hat Pulse on a Single-Period Line

A this point we are equipped to analyze a dispersion relation and produce an answer for minimum acceptable pulse length. Let us consider the simplest of dispersion relations, for a single period line,

$$\cos\theta = \frac{\omega_0^2 - \omega^2}{\kappa},$$

(The development of this relation is reviewed in the next section). We treat the coupling factor κ as a constant. The cell resonance frequency is ω_0, and θ is the phase advance per cell. The group velocity is determined from

$$\theta' = \frac{2\omega}{\kappa \sin\theta},$$

according to

$$\frac{V_g}{c} = \beta_g = \frac{L}{c}\frac{1}{\theta'},$$

with *L* the cell period. In fact, having chosen $L = \lambda 2^{-1/2}$,

$$\beta_g = 2^{1/2}\pi\left(\frac{d\theta}{d\ln\omega}\right)^{-1}, \qquad \text{or} \qquad \theta' = \frac{2^{1/2}\pi}{\beta_g \omega}$$

We treat group velocity and phase-advance per cell as inputs. The quantity ω_0 amounts to a choice of units for frequency, and κ is derived from θ and θ'. With two more differentiations one can show that the condition for zero first order dispersion is

$$\tan\theta = \omega\theta' = \frac{2^{1/2}\pi}{\beta_g},$$

and this implies that phase-advance per cell is fixed, and, for low group velocity, near $\pm\pi/2$, modulo π (*i.e.*, mid-band). For example, phase advance per cell is 88.1° for 0.15c group velocity, and 89.1° for 0.0677c. One can show after some algebra that with this choice of phase-advance per cell,

$$\theta''' = (\theta')^3 \sin\theta \approx \left(\frac{2^{1/2}\pi}{\beta_g\omega}\right)^3.$$

Our dispersion formulae call on the cumulative phase-shift to a point z,

$$\Theta''' = N\theta''' = \left(\frac{2^{1/2}\pi N^{1/3}}{\beta_g\omega}\right)^3,$$

and we take the point $z=NL=L_S$ at the last cell of the secondary line, with N˜50. Our normalized time coordinate is

$$\hat{\tau} = \left(\frac{2}{\Theta'''}\right)^{1/3}\tau = \frac{\beta_g\omega\tau}{2^{1/6}\pi N^{1/3}},$$

and our normalized pulse length is

$$\hat{T}_p = \left(\frac{2}{\Theta'''}\right)^{1/3}T_p = \frac{\beta_g\omega T_p}{2^{1/6}\pi N^{1/3}}.$$

We can evaluate this directly, for 0.15c group velocity,

$$\hat{T}_p = \beta_g 2^{5/6}\frac{f T_p}{N^{1/3}} = \frac{0.15\times 1.78\times 91.39GHz\times 0.3ns}{50^{1/3}} = 1.99,$$

for $0.114c$, $\hat{T}_p = 1.51$ and for 0.0677c, $\hat{T}_p = 0.9$. To maintain $\hat{T}_p \geq 2.3$ one requires group velocity of $0.17c$ or higher. In summary, for a line with second-order dispersion dominated transport, we require

$$\beta_g \geq 1.3\frac{N^{1/3}}{f T_p}.$$

We can produce a similar result for a first-order line, using

$$\theta'' = \frac{L^2}{c^2}\frac{1}{\beta_g^2}\left(\frac{\beta_g}{\varphi} - \cot\theta\right),$$

with

$$\varphi = \frac{\omega L}{c}.$$

The result is

$$\hat{T}_p = \frac{cT_p\beta_g}{(\pi N)^{1/2} L}\left|\frac{\beta_g}{\varphi} - \cot\theta\right|^{-1/2} > 1.46.$$

So for example, in a $2\pi/3$ mode synchronous structure, one would require,

$$\beta_g > 0.66\frac{N^{1/2}}{f\,T_p}.$$

For our parameters this would correspond to a group velocity of $0.17c$ or higher.

2.2 Coupled-Cavity Formulation

A more resilient approach to the problem models the secondary line as a chain of $n=1,2,...N$ coupled cavities. For cell voltage in cell $n\neq 1,N$, the model takes the form,

$$\left(\frac{\partial^2}{\partial t^2} + \frac{\omega_n}{Q_n}\frac{\partial}{\partial t} + \omega_n^2\right)V_n = \frac{1}{2}\omega_n^2\left(\kappa_{n-1/2}V_{n-1} + \kappa_{n+1/2}V_{n+1}\right).$$

In steady-state, at constant angular frequency ω, this is

$$\left(j\frac{\omega\omega_n}{Q_n} + \omega_n^2 - \omega^2\right)\tilde{V}_n = \frac{1}{2}\omega_n^2\left(\kappa_{n-1/2}\tilde{V}_{n-1} + \kappa_{n+1/2}\tilde{V}_{n+1}\right).$$

Constant-Phase Advance Per Cell

Before considering the general case, let us review the problem of a line tapered in such a way as to permit constant voltage amplitude along the line, with a prescribed constant phase-shift per cell, θ. This corresponds to the conventional "constant-gradient" structure. The voltage phasor in the n-th cavity is,

$$\tilde{V}_n = \tilde{V}_0 e^{-jn\theta}.$$

In later work, we can return to consider more general lines, as these assumptions are not apriori necessary, and therefore may deviate from the optimal. They do simplify the problem considerably, however, for we then have the simply relation

$$j\frac{\omega\omega_n}{Q_n} + \omega_n^2 - \omega^2 = \frac{1}{2}\omega_n^2\left(\kappa_{n-1/2}e^{j\theta} + \kappa_{n+1/2}e^{-j\theta}\right).$$

determining,

$$\omega_n^2 - \omega^2 = \omega_n^2 \kappa_n \cos\theta, \qquad \frac{\omega\omega_n}{Q_n} = \frac{1}{2}\omega_n^2\left(\kappa_{n-1/2} - \kappa_{n+1/2}\right)\sin\theta,$$

where we define,

$$\kappa_n \equiv \frac{1}{2}\left(\kappa_{n-1/2} + \kappa_{n+1/2}\right).$$

These relations permit us to compute the group velocity,

$$\beta_{gn} = \frac{1}{2}\varphi\kappa_n\left(\frac{\omega_n}{\omega}\right)^2 \sin\theta,$$

with

$$\varphi = \frac{\omega L}{c}.$$

This permits us to solve for the cell frequencies in terms of θ, φ and β_g, and the desired operating angular frequency, ω,

$$\frac{\omega_n^2}{\omega^2} = 1 + 2\frac{\cot\theta}{\varphi}\beta_{gn}, \qquad \Leftrightarrow \qquad \omega_n = \frac{\omega}{\sqrt{1-\kappa_n\cos\theta_n}}$$

$$\kappa_n = \frac{\beta_{gn}}{\beta_{gn}\cos\theta + \frac{1}{2}\varphi\sin\theta}.$$

The Q value for these interior cells is that due to wall losses alone and we will take it to be a constant Q_w~2700, as for the optimized closed pillbox. If the group velocity profile has been chosen correctly it should result that the coupling constants satisfy

$$\kappa_{n-1/2} = \kappa_{n+1/2} + \frac{2}{Q_w\sin\theta}\left(\frac{\omega}{\omega_n}\right).$$

to a good approximation.

The voltage in the input cell satisfies,

$$\left(\frac{\partial^2}{\partial t^2} + \frac{\omega_1}{Q_1}\frac{\partial}{\partial t} + \omega_1^2\right)V_1 = \frac{1}{2}\omega_1^2\kappa_c V_2 + 2\frac{\omega_1}{Q_{e1}}\frac{\partial V_F}{\partial t},$$

where forward-going voltage in the connecting guide has been transformed to to V_F, and reverse waveform V_R, satisfying (continuity of tangential electric field),

$$V_1 = V_F + V_R.$$

The loaded Q of the first cell is

$$\frac{1}{Q_1} = \frac{1}{Q_{e1}} + \frac{1}{Q_{w1}}.$$

The input cell resonance frequency, and external Q, Q_{e1} are adjusted to insure no reflected signal in steady-state ($V_1 = V_F$), corresponding to a match on the transmission line to a forward-wave with phase-advance per cell θ. Thus

$$j\frac{\omega\omega_1}{Q_1} + \omega_1^2 - \omega^2 = \frac{1}{2}\omega_1^2 \kappa_i e^{-j\theta} + 2j\frac{\omega\omega_1}{Q_{e1}},$$

This permits us to solve for the input coupler cell parameters,

$$\frac{1}{Q_{e1}} = \frac{1}{Q_w} + \frac{1}{2}\frac{\omega_1}{\omega}\kappa_i \sin\theta, \qquad \frac{\omega_1}{\omega} = \frac{1}{\sqrt{1 - \frac{1}{2}\kappa_i \cos\theta}}.$$

The condition on external Q amounts to the statement that power should be flowing into the first cell from the connecting guide at the same rate at which it is leaving the first cell (some going into the wall and most going into the next cell).

As for the determination of κ_c, there are two distinguished choices. If the first iris radius is desired to match the other cells in dimension, it may be determined from the group velocity profile, so that $\kappa_i = \kappa_{3/2}$. Alternatively, we may ask that the coupler cavity be driven as though it were part of an infinite structure. In this case, the natural resonance frequency of the first cavity should be the same as those nearby, so that $\kappa_i = 2\kappa_{3/2}$.With this choice, the drive to the cavity and the coupling from cell #2 add in such a way as to mimic the drive from two adjacent cells,

$$\frac{1}{2}\omega_1^2 \kappa_i e^{-j\theta} + 2j\frac{\omega\omega_1}{Q_{e1}} \approx \kappa_{3/2}\omega_1^2 \cos\theta,$$

and the imaginary part is satisfied approximately for high Q_w.

The voltage in the output cell evolves according to

$$\left(\frac{\partial^2}{\partial t^2} + \frac{\omega_N}{Q_N}\frac{\partial}{\partial t} + \omega_N^2\right)V_N = \frac{1}{2}\omega_N^2 \kappa_o V_{N-1},$$

and the absence of a drive term corresponds to the assumption that the waveguide connecting to the output cell is terminated in a matched load. The condition for match to a forward wave with the prescribed phase-advance per cell is,

$$j\frac{\omega\omega_N}{Q_N} + \omega_N^2 - \omega^2 = \frac{1}{2}\omega_N^2 \kappa_o e^{j\theta},$$

so that

$$\frac{\omega_N}{\omega} = \frac{1}{\sqrt{1 - \frac{1}{2}\kappa_o \cos\theta}}, \qquad \frac{1}{Q_{eN}} = -\frac{1}{Q_w} + \frac{1}{2}\frac{\omega_N}{\omega}\kappa_o \sin\theta.$$

Notice the implied lower bound on the coupling constant,

$$\kappa_o > 2\frac{\omega}{\omega_N}\frac{1}{Q_w \sin\theta}.$$

The natural choices for the coupling constant to the output cell are $\kappa_o = \kappa_{N-1/2}$, and $\kappa_o = 2\kappa_{N-1/2}$.

In general, our problem is a bit more complicated, as we would like to consider examples where the first-order dispersion vanishe. In the continuum case, the condition for this required phase-advance related to group velocity, and yet our group velocity is tapered. On the other hand, we also noticed that the phase-advance per cell did not change greatly, being near mid-band at $\theta=\pi/2$. Thus in the simplest approximation, we would take

$$\tan\theta(z) = \frac{\varphi}{\beta_g(z)} = \frac{\omega L}{V_g(z)}, \qquad (*)$$

or perhaps, even constant at $\pi/2$. While this is clearly straightforward to implement, we would like nevertheless to have a more rigorous algorithm.

Tapered Phase-Advance Per Cell

Let us perform a similar analysis for tapered phase-advance per cell. We suppose,

$$\tilde{V}_n = \tilde{V}_0 e^{-j\Phi_n},$$

and denote

$$\Delta_{n-1/2} = \Phi_n - \Phi_{n-1},$$

so that, for interior cells,

$$j\frac{\omega\omega_n}{Q_n} + \omega_n^2 - \omega^2 = \frac{1}{2}\omega_n^2\left(\kappa_{n-1/2}e^{j\Delta_{n-1/2}} + \kappa_{n+1/2}e^{-j\Delta_{n+1/2}}\right).$$

determining,

$$\omega_n^2 - \omega^2 = \frac{1}{2}\omega_n^2\left(\kappa_{n-1/2}\cos\Delta_{n-1/2} + \kappa_{n+1/2}\cos\Delta_{n+1/2}\right), \qquad \text{(dispersion relation)}$$

$$\frac{\omega\omega_n}{Q_n} = \frac{1}{2}\omega_n^2\left(\kappa_{n-1/2}\sin\Delta_{n-1/2} - \kappa_{n+1/2}\sin\Delta_{n+1/2}\right). \qquad \text{(constant amplitude)}$$

With this we may express,

$$\frac{4}{\varphi}\frac{\omega^2}{\omega_n^2} = \frac{\kappa_{n-1/2}\sin\Delta_{n-1/2}}{\beta_{g\,n-1/2}} + \frac{\kappa_{n+1/2}\sin\Delta_{n+1/2}}{\beta_{g\,n+1/2}},$$

in terms of the the local group velocity

$$\beta_{g\,n-1/2} = \frac{L}{c}\left(\frac{\partial\Delta_{n-1/2}}{\partial\omega}\right)^{-1},$$

with L the cell-period (assumed constant).

The voltage in the input cell satisfies,

$$j\frac{\omega\omega_1}{Q_1}+\omega_1^2-\omega^2=\frac{1}{2}\omega_1^2\kappa_i e^{-j\Delta_{3/2}}+2j\frac{\omega\omega_1}{Q_{e1}},$$

so that

$$\frac{1}{Q_{e1}}=\frac{1}{Q_w}+\frac{1}{2}\frac{\omega_1}{\omega}\kappa_i\sin\Delta_{3/2},\qquad\qquad \frac{\omega_1}{\omega}=\frac{1}{\sqrt{1-\frac{1}{2}\kappa_i\cos\Delta_{3/2}}}.$$

The voltage in the output cell satisfies

$$j\frac{\omega\omega_N}{Q_N}+\omega_N^2-\omega^2=\frac{1}{2}\omega_N^2\kappa_o e^{j\Delta_{N-1/2}},$$

so that

$$\frac{\omega_N}{\omega}=\frac{1}{\sqrt{1-\frac{1}{2}\kappa_o\cos\Delta_{N-1/2}}},\qquad \frac{1}{Q_{eN}}=-\frac{1}{Q_w}+\frac{1}{2}\frac{\omega_N}{\omega}\kappa_o\sin\Delta_{N-1/2}.$$

Since we are at this point somewhat removed from the original continuum picture of a uniform line, let us return to reflect on the propagation characteristics in a tapered line. In the time-domain, the voltage at the n-th cell can be obtained by an inverse Fourier transformation,

$$V_n(t)=\int_{-\infty}^{+\infty}\frac{d\omega}{\sqrt{2\pi}}\tilde{V}_0(\omega)\exp\big(j\omega t-\Phi_n(\omega)\big).$$

Analyzing this in the manner of the foregoing sections, one can see that the group delay for arrival of a waveform at cell #n is

$$\tau_n=\frac{\partial\Phi_n}{\partial\omega},\qquad\Leftrightarrow\qquad \tau_n-\tau_{n-1}=\frac{\partial\Delta_{n-1/2}}{\partial\omega},$$

evaluated at the design drive frequency. Thus the expression for local group velocity employed above can be interpreted as the velocity of propagation from cell *n-1* to cell *n*. The requirement for zero first order dispersion at cell *n* is

$$\frac{\partial^2\Phi_n}{\partial\omega^2}=0,$$

evaluated at the design operating frequency. To make this explicit, we differentiate the dispersion relation once

$$4\frac{\omega}{\omega_n^2}=\kappa_{n-1/2}\sin\Delta_{n-1/2}\frac{\partial\Delta_{n-1/2}}{\partial\omega}+\kappa_{n+1/2}\sin\Delta_{n+1/2}\frac{\partial\Delta_{n+1/2}}{\partial\omega},$$

(just the expression above with group velocity), and again,

$$\frac{4}{\omega_n^2} = \kappa_{n-1/2}\cos\Delta_{n-1/2}\left(\frac{\partial\Delta_{n-1/2}}{\partial\omega}\right)^2 + \kappa_{n+1/2}\cos\Delta_{n+1/2}\left(\frac{\partial\Delta_{n+1/2}}{\partial\omega}\right)^2.$$

We may express our system of equations in terms of

$$C_{n+1/2} = \kappa_{n+1/2}\cos\Delta_{n+1/2},$$
$$S_{n+1/2} = \kappa_{n+1/2}\sin\Delta_{n+1/2},$$

so that

$$\omega_n^2 - \omega^2 = \frac{1}{2}\omega_n^2\left(C_{n+1/2} + C_{n-1/2}\right), \qquad \text{(dispersion relation)}$$
$$\frac{\omega\omega_n}{Q_w} = \frac{1}{2}\omega_n^2\left(S_{n-1/2} - S_{n+1/2}\right), \qquad \text{(constant amplitude)}$$
$$\frac{4}{\varphi}\frac{\omega^2}{\omega_n^2} = \frac{S_{n-1/2}}{\beta_{g\,n-1/2}} + \frac{S_{n+1/2}}{\beta_{g\,n+1/2}}, \qquad \text{(group velocity)}$$
$$\frac{4}{\varphi^2}\frac{\omega^2}{\omega_n^2} = \frac{C_{n-1/2}}{\beta_{g\,n-1/2}^2} + \frac{C_{n+1/2}}{\beta_{g\,n+1/2}^2}. \qquad \text{(zero first order dispersion)}$$

In the first approximation, we can interpolate to obtain

$$\frac{2}{\varphi}\frac{\omega^2}{\omega_n^2} = \frac{S_n}{\beta_{g\,n}}, \qquad \frac{2}{\varphi^2}\frac{\omega^2}{\omega_n^2} = \frac{C_n}{\beta_{g\,n}^2}, \qquad 1 - \frac{\omega^2}{\omega_n^2} = C_n,$$

from which we obtain

$$\frac{\omega}{\omega_n} = \left(1 + 2\frac{\beta_{g\,n}^2}{\varphi^2}\right)^{-1/2}, \quad S_n = \frac{2\beta_{g\,n}}{\varphi}\left(1 + 2\frac{\beta_{g\,n}^2}{\varphi^2}\right)^{-1}, \quad C_n = \frac{2\beta_{g\,n}^2}{\varphi^2}\left(1 + 2\frac{\beta_{g\,n}^2}{\varphi^2}\right)^{-1}.$$

For a prescribed value for $\beta_{g\,3/2}$ (*e.g.*, interpolated from the desired profile $\beta_{g\,n+1/2} = \beta_g\,(z = nL)$), these relations determine $S_{3/2}$, and $C_{3/2}$, and all the cell resonance frequencies ω_n. We elect to accept these values and compute the coupling contstants required on the remainder of the line to maintain constant amplitude and zero first order dispersion. This procedure works at the expense of a small deviation from the desired group velocity profile; we have no particular requirement on the absolute value of the phase-advance per cell since we have no synchronism requirement. Constant amplitude is insured by

$$S_{n+1/2} = S_{n-1/2} + \frac{2}{Q_w}\frac{\omega}{\omega_n},$$

and provides a collection of coefficients $S_{n-1/2}$. Defining

$$\gamma_{n-1/2} = \frac{S_{n-1/2}}{\beta_{g\,n-1/2}},$$

$\gamma_{3/2}$ is known, and one may solve for the group velocity coefficients,

$$\gamma_{n+1/2} = \frac{4}{\varphi}\frac{\omega^2}{\omega_n^2} - \gamma_{n-1/2} \qquad \Rightarrow \qquad \beta_{g\,n-1/2} = \frac{S_{n-1/2}}{\gamma_{n-1/2}}.$$

Defining

$$\Gamma_{n-1/2} = \frac{C_{n-1/2}}{\beta_{g\,n-1/2}^2},$$

$\Gamma_{3/2}$ is known, and one may solve for

$$\Gamma_{n+1/2} = \frac{4}{\varphi^2}\frac{\omega^2}{\omega_n^2} - \Gamma_{n-1/2} \qquad \Rightarrow \qquad C_{n-1/2} = \Gamma_{n-1/2}\beta_{g\,n-1/2}^2.$$

In this way, we obtain

$$\kappa_{n-1/2} = \left(C_{n-1/2}^2 + S_{n-1/2}^2\right)^{1/2}. \qquad (**)$$

A more rigorous approach, respecting the required dispersion relation is

$$C_{n-1/2} = \frac{\dfrac{2}{\varphi^2}\dfrac{\omega^2}{\omega_n^2} - \dfrac{1}{\beta_{g\,n+1/2}^2}\left(1 - \dfrac{\omega^2}{\omega_n^2}\right)}{\left(\dfrac{1}{\beta_{g\,n+1/2}^2} - \dfrac{1}{\beta_{g\,n-1/2}^2}\right)},$$

however, this reduces to

$$C_{n-1/2} = 2\frac{\beta_{g\,n+1/2}^2}{\varphi^2}\frac{1}{1+2\dfrac{\beta_{g0\,n-1/2}^2}{\varphi^2}}\frac{1-\dfrac{\beta_{g0\,n-1/2}^2}{\beta_{g\,n+1/2}^2}}{1-\dfrac{\beta_{g\,n+1/2}^2}{\beta_{g\,n-1/2}^2}}, \qquad (***)$$

with $\beta_{g0\,n-1/2}$ the initial estimate for the group velocity. Numerically, this must be evaluated carefully to avoid roundoff.

2.3 Numerical Algorithms for Coupled-Cavity Solvers

For simulation of bench measurements we will solve these coupled oscillator equations in the frequency domain. For calculation of transient waveforms we will solve them in the time-domain For clarity we set down the numerical formalisms employed in either case. The coupled circuit model consists of *N* 2nd order differential equations,

$$\left(\frac{\partial^2}{\partial t^2}+\frac{\omega_n}{Q_n}\frac{\partial}{\partial t}+\omega_n^2\right)V_n=\frac{1}{2}\omega_n^2\left(\kappa_{n-1/2}V_{n-1}+\kappa_{n+1/2}V_{n+1}\right)+\frac{2\omega_{en}}{Q_n}\frac{\partial V_F}{\partial t}\delta_{n,1},$$

with $\delta_{n,m}$ the Kronecker delta function, $\delta_{n,m}=0$ unless *n*=*m*, in which case $\delta_{n,m}=1$. In the frequency domain at drive frequency Ω, we have

$$-\frac{1}{2}\omega_n^2\kappa_{n-1/2}\tilde{V}_{n-1}+\left(j\Omega\frac{\omega_n}{Q_n}+\omega_n^2-\Omega^2\right)\tilde{V}_n-\frac{1}{2}\omega_n^2\kappa_{n+1/2}\tilde{V}_{n+1}=2j\Omega\frac{\omega_{en}}{Q_n}\tilde{V}_F\delta_{n,1}.$$

This is a tri-diagonal matrix equation and may be inverted quickly, using, for example, the subroutine tridag from *Numerical Recipes*.[2] In this way one can quickly compute,

$$S_{11}(\Omega)=\frac{\tilde{V}_1(\Omega)}{\tilde{V}_F(\Omega)}-1,\qquad S_{21}(\Omega)=\frac{\tilde{V}_N(\Omega)}{\tilde{V}_F(\Omega)}.$$

In a similar fashion, adding a drive to the output cell, one can compute S_{21}, and S_{22}.

In the time-domain one may solve the second-order equations directly, or make an eikonal approximation, preferred for the speed of calculation. In the first case one writes the equations as

$$W_n=\frac{\partial V_n}{\partial t},$$

$$\frac{\partial W_n}{\partial t}=-\frac{\omega_n}{Q_n}W_n-\omega_n^2V_n+\frac{1}{2}\omega_n^2\left(\kappa_{n-1/2}V_{n-1}+\kappa_{n+1/2}V_{n+1}\right)+\frac{2\omega_{en}}{Q_n}\frac{\partial V_F}{\partial t}\delta_{n,1},$$

and proceeds to a discrete time step, using a leap-frog approach, where *W* is computed at midpoints $t_{l+1/2}$, and *V* is computed at the time-centered points t_l. Thus

$$W_n^{l+1/2}=\frac{V_n^{l+1}-V_n^l}{\Delta t},$$

$$\frac{W_n^{l+1/2}-W_n^{l-1/2}}{\Delta t}=-\frac{\omega_n}{Q_n}\frac{W_n^{l+1/2}+W_n^{l-1/2}}{2}-\omega_n^2\left(V_n^l-\tfrac{\kappa_{n-1/2}}{2}V_{n-1}^l-\tfrac{\kappa_{n+1/2}}{2}V_{n+1}^l\right)+\frac{2\omega_{en}}{Q_n}\frac{\partial V_F}{\partial t}(t_l)\delta_{n,1}.$$

More explicitly, starting at time t_l, with $W_n^{l-1/2}$, V_n^l known, one proceeds to the next time step using,

$$W_n^{l+1/2}=\left(\frac{1-\frac{\omega_n\Delta t}{2Q_n}}{1+\frac{\omega_n\Delta t}{2Q_n}}\right)W_n^{l-1/2}-\frac{D_n^l\Delta t}{\left(1+\frac{\omega_n\Delta t}{2Q_n}\right)},$$

$$V_n^{l+1} = V_n^l + W_n^{l+1/2}\Delta t,$$

where we abbreviate

$$D_n^l = \omega_n^2\left(V_n^l - \tfrac{\kappa_{n-1/2}}{2}V_{n-1}^l - \tfrac{\kappa_{n+1/2}}{2}V_{n+1}^l\right) + \frac{2\omega_n}{Q_{en}}\frac{\partial V_F}{\partial t}(t_l)\delta_{n,1}.$$

This approach requires 60 steps per rf period and is unnecessarily time-consuming for a narrow band drive. This approach is useful, however, as a check of the following eikonal (or "WKB") technique in the case of a short pulse excitation.

In the eikonal approach we assume a narrow band rf drive taking the form,

$$V_F(t) = \Re\left\{\tilde{V}_F(t)e^{j\Omega t}\right\},$$

where "narrow-band" means,

$$\left|\frac{\partial\tilde{V}_F}{\partial t}\right| << \Omega\left|\tilde{V}_F\right|.$$

We look for a solution for cell voltages taking the like form of slowly varying phasor amplitudes at the carrier frequency *W*,

$$2j\Omega\frac{\partial\tilde{V}_n}{\partial t} + \left(j\Omega\frac{\omega_n}{Q_n} + \omega_n^2 - \Omega^2\right)\tilde{V}_n = \frac{1}{2}\omega_n^2\left(\kappa_{n-1/2}\tilde{V}_{n-1} + \kappa_{n+1/2}\tilde{V}_{n+1}\right) + \frac{2j\Omega\omega_{en}}{Q_n}\tilde{V}_F\delta_{n,1}.$$

Letting,

$$\Delta_n = j\Omega\frac{\omega_n}{Q_n} + \omega_n^2 - \Omega^2,$$

the time-centered discrete form of the equations for *n*-th cell voltage at time step *a*, $\tilde{V}_n^a$, is

$$2j\Omega\frac{\tilde{V}_n^{a+1} - \tilde{V}_n^a}{\Delta t} + \Delta_n\frac{\tilde{V}_n^{a+1} + \tilde{V}_n^a}{2} = \frac{1}{2}\omega_n^2\left(\kappa_{n-1/2}\frac{\tilde{V}_{n-1}^{a+1} + \tilde{V}_{n-1}^a}{2} + \kappa_{n+1/2}\frac{\tilde{V}_{n+1}^{a+1} + \tilde{V}_{n+1}^a}{2}\right), + \frac{2j\Omega\omega_{en}}{Q_n}\tilde{V}_F^a\delta_{n,1}$$

and this may be rewritten as,

$$-\frac{1}{4}\omega_n^2\kappa_{n-1/2}\tilde{V}_{n-1}^{a+1} + \left(\frac{2j\Omega}{\Delta t} + \frac{\Delta_n}{2}\right)\tilde{V}_n^{a+1} - \frac{1}{4}\omega_n^2\kappa_{n+1/2}\tilde{V}_{n+1}^{a+1} =$$
$$\frac{1}{4}\omega_n^2\kappa_{n-1/2}\tilde{V}_{n-1}^{a+1} + \left(\frac{2j\Omega}{\Delta t} - \frac{\Delta_n}{2}\right)\tilde{V}_n^{a+1} + \frac{1}{4}\omega_n^2\kappa_{n+1/2}\tilde{V}_{n+1}^{a+1} + \frac{2j\Omega\omega_{en}}{Q_n}\tilde{V}_F^a\delta_{n,1}.$$

Thus the eikonal form of the equations can be solved by a time-centered difference and one tri-diagonal matrix inversion at each time-step. Since the number of time-steps is governed only by the structure and drive bandwidths, this approach can be much faster than solution of the full 2nd order system.

2.4 Numerical Examples

I have written a code `NMAT` to setup a structure circuit, compute the results of *S*-matrix measurements on it, and compute transient wave propagation down the circuit. The code is described at greater length in another note (on the subject of S-matrix measurements). Here I include simply an input file with some annotations

Table 1. Parameters for the constant impedance implementation of the secondary.

`$INPUTNML`	
`iphase=1`	*phase-advance option...* *0=synchronous phase advance,* *1=zero 1st order dispersion according to Eq. (*)* *2=fixed phase-advance* *3=zero 1st order dispersion according to Eq. (**)* *4=zero 1st order dispersion according to Eq. (***)*
`idopt=0,`	*if≠0, optimize coupler cell parameters*
`bphase=90.`	*used if* `iphase`=2
`qw0=2700.`	*wall* Q *of a secondary line cavity*
`iopt=2`	*primary waveform option...* *0=inject an exponentially decaying waveform* *1=inject a "cw" pulse with step turn on* *2=inject a square pulse*
`tfw=3.e-10`	*full-width square pulse, used if* `iopt=2`
`qep=100.`	*loaded* Q *for exponent. drive,* `iopt=0`
`qem=0.`	*if ≠ 0, use for external* Q*, last cell*
`idetune=0`	*if ≠ 0, don't detune coupler cells*
`ireadat=0`	*if ≠ 0, read data file for overlay*
`ncell=50,`	*number of cells secondary*
`xcell=0.2319`	*cell length secondary*
`ibeta=0`	*group velocity taper option...* *0=use* `beta1` *1=compute constant gradient taper* *2=constant impedance*
`beta0=0.174`	*initial* V_g/c *secondary*
`beta1=0.174`	*final* V_g/c *secondary , if* `ibeta=0`
`freq0=91.392e9`	*design operating frequency*
`fbase=91.392e9`	*carrier frequency (a numerical parameter)*
`tmin=0.,`	*time starts here, sec*
`tmax=10.e-9,`	*time ends here, sec*
`tswitch=1.e-10`	*primary switched at this time >* `tmin`
`ntin=2000`	*number of time steps*
`imovie=0,`	*0=no movie, else movie*
`iplot=0,`	*0=mostly no plots, 1=lots of plots*
`isolve=0,`	0=eikonal solve, 1 integrate exactly
`imodes=0,`	1=plot modes (if iplot ne 0)
`$END`	

Infinite *Q*, Constant Impedance, Zero Dipersion

The first simplest thing to do with such a code is to compare directly with the case of a lossless transmission line, with zero first-order dispersion. We do this for the parameters listed in Table 1, with the wall *Q* of 2700 replaced by 2.7×10^9. The result is depicted in Fig. 14. At first this seems a little bit disappointing as the parameters should correspond to unit amplitude in the output cell, according to the results of the Airy function analysis. The problem is seen in Fig. 15, depicting the voltage in the penultimate cavity; this is too large, indicative of a match at the output that is not sufficiently broadband.

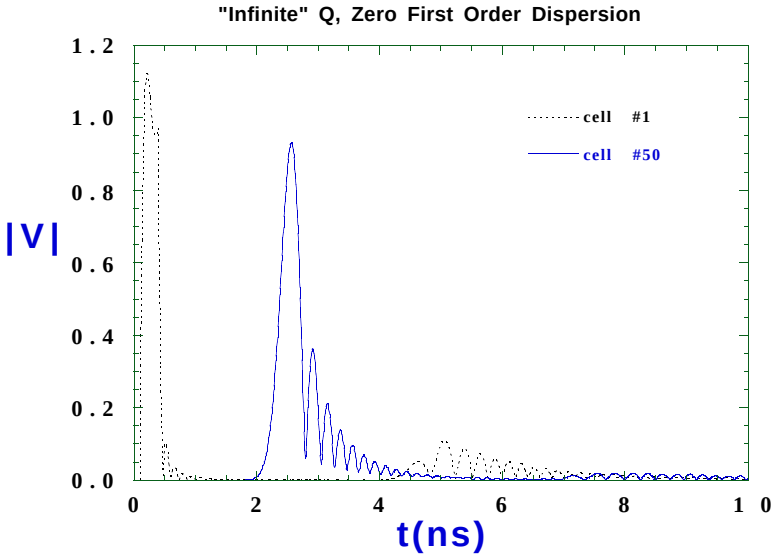

Figure 14. Test-case of a 0.174c, 50 cell, near π/2 phase advance line, subject to a 300ps unit amplitude incident pulse. The response of the first cavity and the last cavity are shown.

Figure15 . Response of the penultimate cavity for the case of Fig. 14.

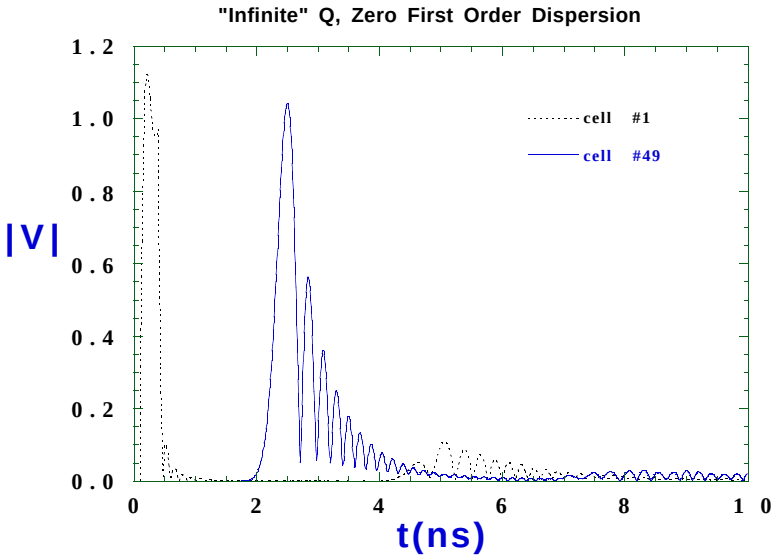

For this case, the coupling constants $\kappa_i = \kappa_{3/2}$ and $\kappa_o = \kappa_{N-1/2}$ were used. I added a subroutine to NMAT to scan choices of input coupler parameters to locate a more broadband match at the ouptut cavity, and it located the value $\kappa_o \approx 2\kappa_{N-1/2}$.

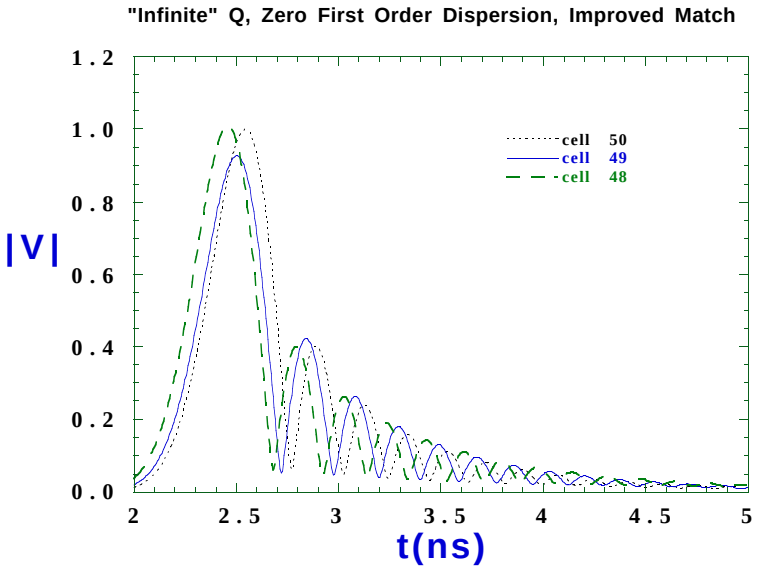

Figure16 . Response of the last three cavities, with a better match on the output, and other parameters as in Table 1, and Figs. 14 and 15.

One can see that the match at the output is a delicate matter, and will require additional attention. Results for this parameter set are summarized in Fig. 16.

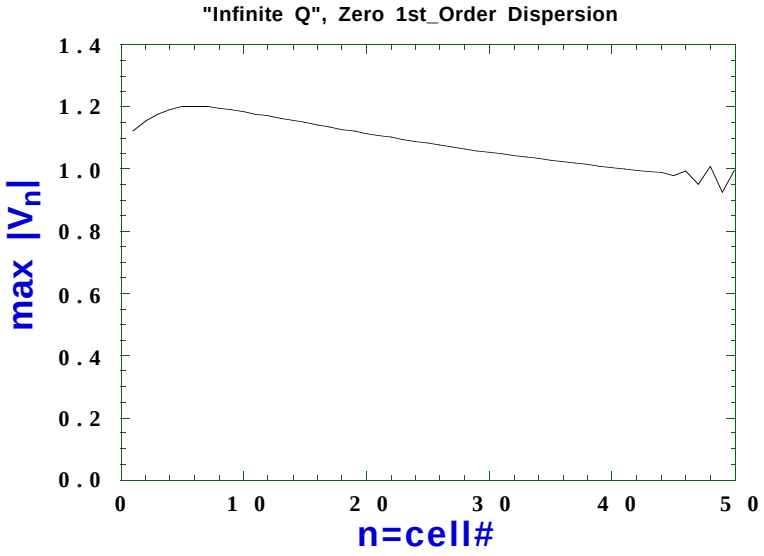

Figure16 . Summary of the results (as in Fig. 16) for all 50 cells, of maximum in voltage (over all time) versus cell number.

Finite *Q*, Constant Impedance, Zero Dispersion

Next we restore the natural wall losses, Q_W~2700 as in Table 1. The result for cell #50 is shown in Fig. 17 and a summary of all cells in Fig. 18.

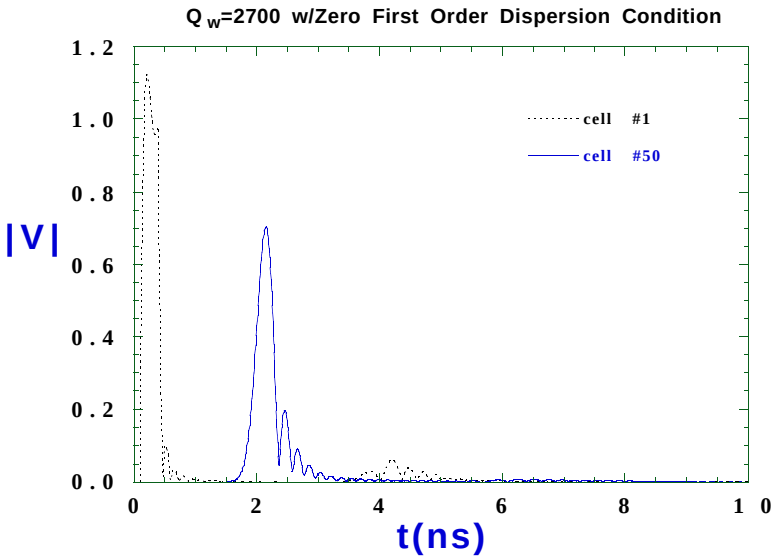

Figure17 . Effect of realistic losses is to attenuate the pulse; parameters are those of Table 1.

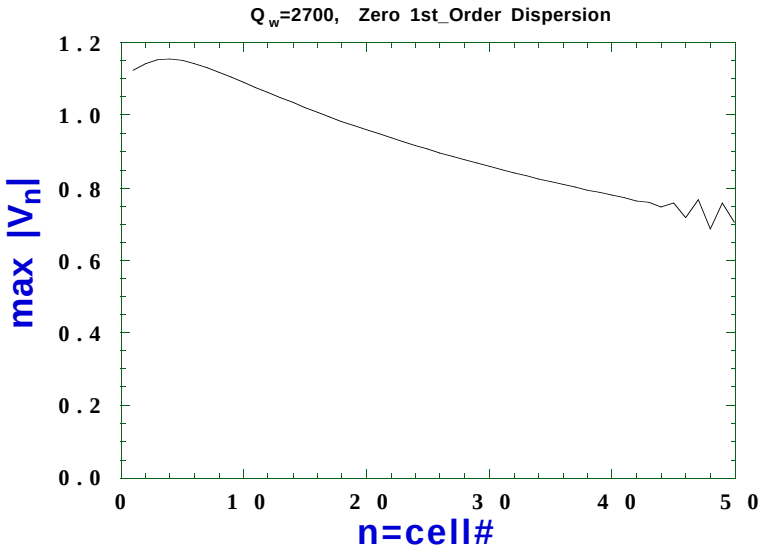

Figure18 . Summary of cell maxima, with Table 1 parameters.

To appreciate the scalings corresponding to these parameters, I include some of the NMAT output to screen.

Table 2. Some enjoyable output from NMAT

```
Using user-specificed vg/c at output "beta1"
will use EIKONAL integration (isolve=0)
generating square pulse full-width (ns)   0.3000000
Primary Subr...
writing plot file primout.dat
 transit angle wL/c (deg) =    254.5017
 cell 1 freq (GHz)            91.46199
 cell 2 freq (GHz)            91.53214
 cell N-1 freq (GHz)          91.53214
 cell N freq (GHz)            91.54026
expected fill time (ns) =    2.222802
initial phase adv per cell (deg)    87.75677
final phase adv per cell (deg)      86.73901
external Q 1st cell, 2ndary =       25.34667
external Q last cell, 2ndary =      17.69132
plotting structure parms vs cell # ...
writing plot file parm.dat
DRIVING INPUT CELL
INPUT CELL  steady-state ref. coeff =   1.2530177E-02
 VSWR looking into this port =    1.025378
 |S21| =   0.6874622
in dB =   -3.255024
S-Matrix - Input Coupler
writing plot file nain.dat
writing tabular (KG) data to
nainkg.dat
tabular (KG) data for analytic comp. to
nainkg1.dat
DRIVING OUTPUT CELL
OUTPUT CELL steady-state ref. coeff =   2.0054007E-02
 VSWR looking into this port =    1.040929
 |S12| =   0.9840981
in dB =  -0.1392323
S-Matrix - Output Coupler
writing plot file naout.dat
writing tabular (KG) data to
naoutkg.dat
tabular (KG) data for analytic comp. to
naoutkg1.dat
Analyzing Time-Domain Data w/ Specified Drive...
cell #            Max V
          1   1.124618
         47  0.7668549
         48  0.6864880
         49  0.7592515
         50  0.7033715
 max V-Last/ max V-First   0.6254314
writing plot file junk.dat
plotting waveforms for structure...
writing plot file str.dat
```

Note that the 3dB insertion loss expected is consistent with the peaking voltage of $0.7 \tilde{} 2^{1/2}$ in the last cell.

Finite *Q*, Constant Gradient, Zero Dispersion

To improve the final cell voltage in the presence of losses, we taper the group velocity. The simplest such taper is a constant gradient taper to 0.092*c*. Results are shown in Figs. 19 and 20.

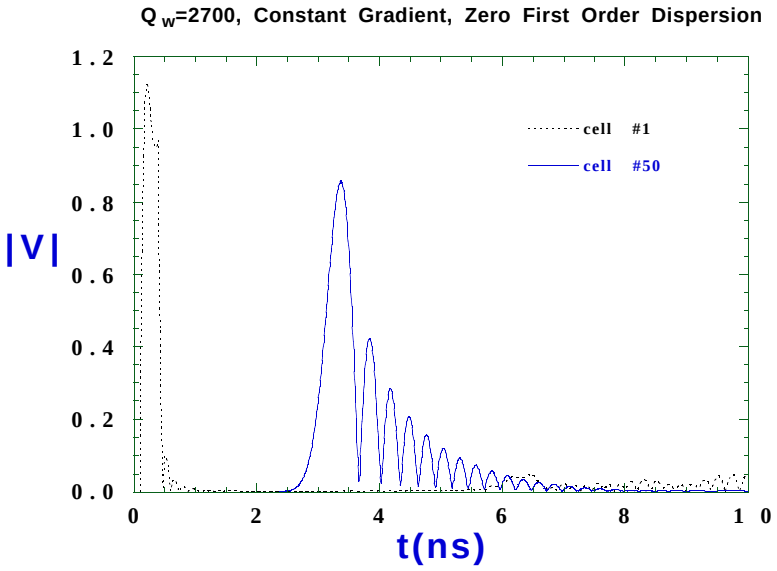

Figure19. Voltage in cell #50 for the "constant gradient" taper.

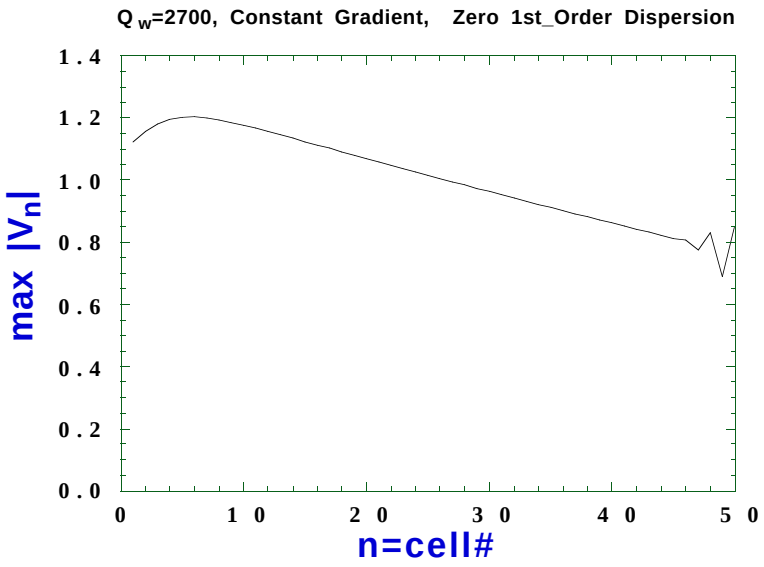

Figure20. Maximum voltage versus cell for the constant gradient case.

This taper corresponds to a voltage of 80% of the initial value and this is not satisfactory. Thus we have more work to do in devising the optimal taper.

Summary of Transient Study

Based on runs with NMAT, it seems that a group velocity below 0.23*c* is possible. It is not yet clear that we can make it to 0.17*c*. In the meantime, it is instructive to make some comparisons of different secondary line designs, to see the effect of dispersion and the various algorithms. These are seen in Fig. 21 and illustrate the importance of operating with a rigorous zeroing of first order dispersion. Eqs. (**) or Eqs. (***) are noticeably better than (*), and much superior to 90° phase-advance, or 1st-order dispersion dominated transport (here illustrated with 120° phase advance).

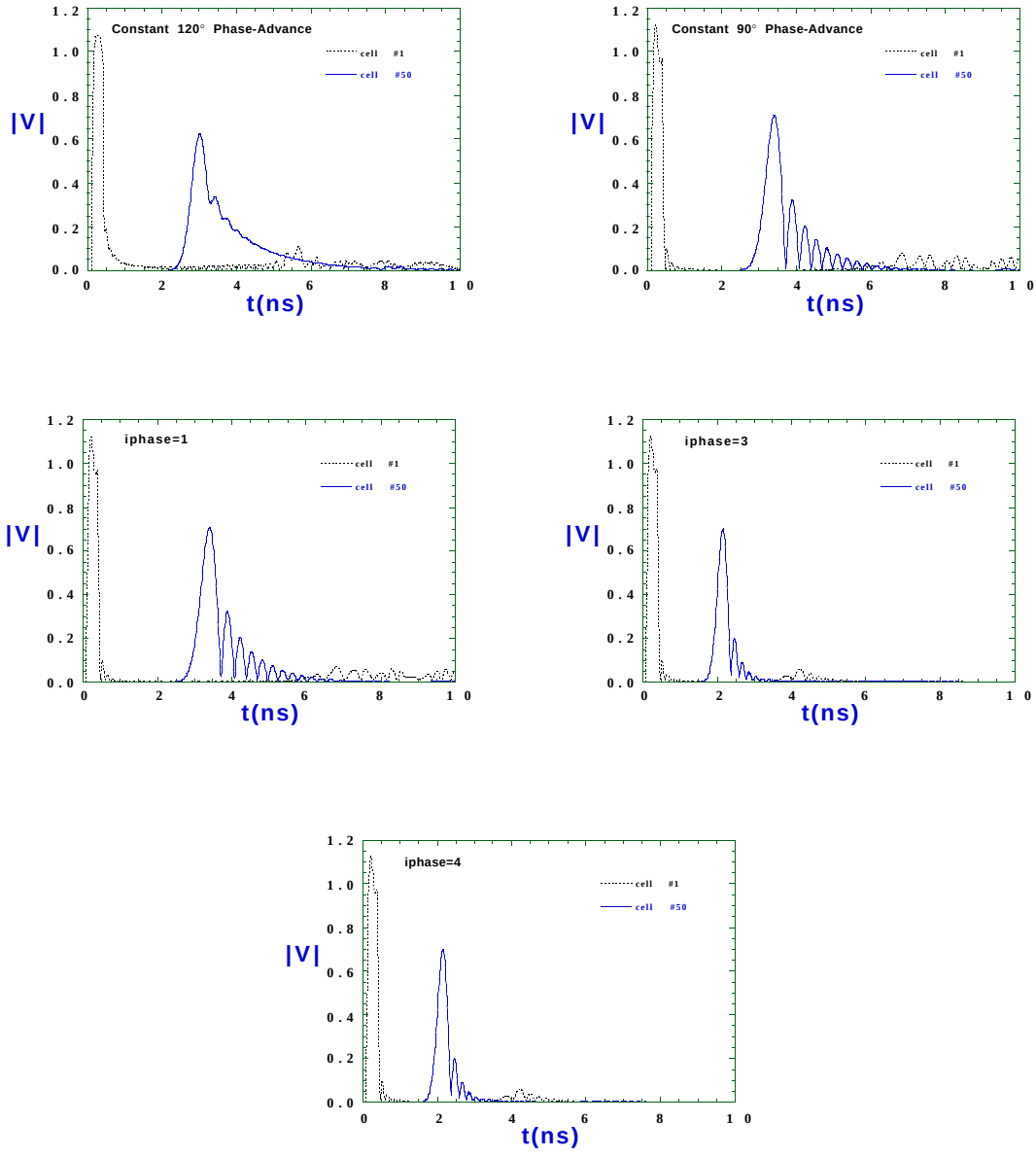

Figure21. Illustrating output waveforms at cell #50 for various tapers.

3. Major Issues to Be Resolved

3.1 Active Switch Material

As to the choice of photoconductor, diamond looks promising. The thermal conductivity of diamond is quite high,

$$\kappa \approx 1500 - 2000 \frac{W}{^\circ K - m}.$$

The bandgap is 5.4eV, so that excitation by 220nm wavelengths or shorter is required. Experience with diamond as a photo-conductor indicates that fields of order 100MV/m-1000MV/m can be held off on a μs time scale. Resistivity is greater than 10^9 Ω-m in the insulating state, and the dielectric constant $\varepsilon \tilde{} 6.7$, with loss tangent $tan\delta < 5x10^{-4}$ at 15 GHz. Temperature coefficient of expansion is $a \tilde{} 2x10^{-6}/°C$. Lee[3] reports for insulating type IIa diamond, a resistivity larger than 10^{14}Ω-m, breakdown field larger than 1GeV/m, and electron and hole mobilities of 1800 and 1200 cm^2V/s. He also notes work of Ho[4] making use of 3rd-harmonic Nd;YAG for excitation.

There appears to be more experience with silicon as a photoconductor. Silicon has a 0.9eV bandgap, thus NdYag (1.06mm) could be used for switching. Hold-off in practice is 6MeV/m on a μs time scale. Skin-depth is 10μm at 10GHz, for a $10^{19}cm^{-3}$ carrier density. Thermal conductivity is 625 W/m-°K.

The laser-requirements for switching require further study. In the meantime, some simple estimates may be helpful as a guide. If we ask that, in the conducting state, the surface resistance be low enough to hold rf dissipation in the photo-conductor to 1% of the total energy in the rf pulse. Then we have

$$P_{diss} \approx \frac{A_T}{A_G} \frac{R_s}{Z_c} P_{rf} \approx 1\% P_{rf},$$

with A_T the surface area of the photoconductor, A_G the waveguide cross-section, and Z_C the characteristic waveguide impedance. Roughly we require a surface resistance of 3.8Ω or lower. This implies a conductivity $4x10^{-4}$ that of copper (and therefore a skin-depth of 44μm), and, if collision time for conduction electrons is comparable to that of copper, we require a conduction electron density lower by the same ratio. In copper the density of conduction band electrons is $8.47x10^{22}cm^{-3}$, so we require $3.8x10^{19}cm^{-3}$. At a minimum this density should be present through, say, 3 skin-depths in the substrate (if such a photon absorption depth can be arranged). Assuming a cross-section of $\lambda^2/2 \tilde{} 5x10^{-2}cm^2$, this is a volume of $7x10^{-4}cm^3$, and a total number of carriers $\tilde{} 3x10^{16}$. If the bandgap is, let us say, 5.5eV, required energy is 24mJ, and fluence is $500mJ/cm^2$. Notice that this laser pulse energy is 14% of the rf energy per secondary. Depending on laser system efficiency, this could be a substantial part of the energy budget for such an accelerator. To emphasize, this estimate assumes an absorption depth in the range of 50μm. This fluence is a nominal value for commercial KrF lasers, which however, have pulse lengths in the 10's of ns range. We will require a pulse length in the ns to ps range. For reference, if the laser energy is delivered in 1ns, the peak power is 20MW. In this case a carrier lifetime of order 1ns is required. Lower fluence might be adequate if plasma formation is assisted by the large field. If, indeed, 1% of the energy is dissipated, this amounts to 1.7mJ in 0.3ns over $5x10^{-2}cm^2$, or a very large $10^{14}W/m^2$. In this case, pulsed temperature rise on the substrate may be computed from

$$\Delta T_{\max}(t) = \frac{2S_{\max}}{\sqrt{\pi\kappa C}} t^{1/2} \approx 6\times 10^4 \,^\circ K \sqrt{\frac{(\kappa C)_{Cu}}{(\kappa C)}}\,.$$

This is excessive and suggests that the actual requirement on surface resistance will arise from thermal stress. In effect, this requires that the electrical conductivity of the substrate be that of copper, reduced by the ratio of the heat capacity-heat conductivity product relative to copper, and corrected for the cyclic stress limit for the substrate.

An alternative is to use a nearly collisionless, switchable dielectric, and preferably one that can be disposed of on each shot, *i.e.*, plasma. The plasma should be sufficiently rarefied that it can be viewed as a dielectric, with

$$\frac{\varepsilon}{\varepsilon_0} = 1 - \frac{\omega_p^2}{\omega^2},$$

with the plasma angular frequency,

$$\omega_p = 5.64\times 10^4 \sqrt{n_p\left(cm^{-3}\right)}.$$

If, for example, we have a length of line *L*, that is a wavelength long,

$$\frac{\omega L}{c} \approx 2\pi,$$

and by switching we change the electrical length by 1/4 wavelength,

$$\sqrt{\omega^2 - \omega_p^2} \approx 2\pi - \frac{\pi}{2},$$

then $\omega_p = 0.5\omega$, and at 91GHz this implies,

$$n_p \approx 2.6\times 10^{13} cm^{-3}.$$

The volume is ~$2\text{x}10^{-2}\text{cm}^3$ and the number of free electrons is ~$5\text{x}10^{11}$, much lower than in the photoconducting case. If each free electron requires of order 5eV (as for example in the organic gases, benzene, diethylaniline, etc.) this amounts to 0.4μJ. For the case of a plasma switch, the matters of vacuum or dielectric tubing to house the plasma should be examined. As a point of reference, if the plasma were produced by 100% ionization of a working gas, the fill pressure would be 0.7mtorr.

3.2 Switch Geometries

The simplest switch geometry appears to be a tee pointing into the substrate, and this feature requires a second depth dimension.

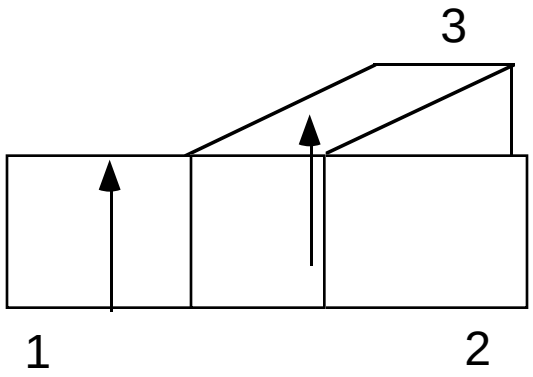

Fig. 8 Symmetric three-port junction.

The S-matrix for the reciprocal three-port junction with reflection symmetry illustrated in Fig. 8, takes the form, after a choice of reference planes,

$$S = \begin{pmatrix} R & T & t \\ T & R & t \\ t & t & r \end{pmatrix},$$

where T and t are real, and unitarity implies

$$R = -\frac{t^2}{2T} + j\sin\mu, \qquad r = \frac{t^2}{2T} - T + j\sin\mu,$$

where,

$$\cos\mu = -T - \frac{t^2}{2T}.$$

In terms of the phase μ, one can show that shorting of port 3 a distance L from the reference plane presents a short to line 1 (or 2) provided,

$$2\beta L = \mu + n\pi,$$

for some integer n. Note that for a diamond fill, dimensions are reduced by about 40% of those in vacuum.

More elaborate geometries are possible, and are of interest where current through the joints (between conductor and switch material) is an issue.

3.3 Sundry Other Problems

Problems raised but not addressed by this analysis include

- Detailed calculations of the geometries required to achieve the desired circuit equivalents.
- Use of a standing-wave cavity for the primary line.
- Material properties of and experience with diamond.

Related problems, having to do with a complete linac system analysis, but bearing directly on the concept are,

- Quadrupole field components, and compensation by dedicated rf quads.
- Optimization, with input from beam dynamics calculations, of the transverse single bunch wakefields
- Cross-talk between beamlines, in higher modes, *i.e.*, the matrix equivalent of multibunch beam break-up.

The first two items above, calculation of copper dimensions, and the standing-wave primary are the subject of two notes nearing completion.

It should be emphasized that the assumed value of single-cell *[R/Q]* of 176Ω and the *Q* of 2700 are in themselves research problems, and the most important at this stage. These figures are equivalent to a per unit length *[R/Q]* of 145kΩ/m, and shunt impedance per unit length of 390MΩ/m. Examples of designs that are close to this have been set down by Henke,[5] (145kΩ/m, Q=2160) and Kang, *et al.*[6] (366 MΩ/m, Q=2460). In the meantime, these values should be considered challenging, particularly since the geometry of interest here is new and different from those considered by previous researchers.

Coupling calculations for secondary and primary cells are important, and GDFIDL, as well as MAFIA will be useful tools for this purpose. In addition, a mode-matching calculator is being prepared for this, and comparisons with the circuit equivalents of Marcuvitz are being studied. For the specific implementation of the primary as illustrated in Fig. 6, the aperture is centered in the guide, of width *d*. The circuit equivalent for this geometry, is a transmission line, periodically loaded with a shunt-susceptance. One may compute this shunt susceptance by considering the somewhat simpler problem of a waveguide of half the width, slit coupled in the broad wall to a waveguide of identical dimension. This work is in progress and results will appear in a separate technical note.

[1] In this connection, see the results for intrinsic efficiency in the technical note on active pulse compression at W-Band.

[2] W.H. Press, S. A. Teukolsky, W. T. Vetterling, and B. P. Flannery, *Numerical Recipes*, The Art of Scientific Computing, (Cambridge University Press, Cambridge, 1992).

[3] Chi H. Lee, *Picosecond Optoelectronic Devices* (Academic Press, New York, 1984)

[4] P.-T. Ho, *et al.*, Opt. Commun. **46**, 202-204.

[5] H. Henke, "mm-Wave Linac and Wiggler Structures"

[6] Y. W. Kang, H. Henke, R. Kustom, F. Mills, and G. Mavrogenes, "A mm-wave Planar Microcavity Structure for Electron Linear Accelerator System", *Proceedings of the 1993 Particle Accelerator Conference* (IEEE, New York, 1993) pp. 549-551.